SANDIA REPORT

SAND2006-5483
Unlimited Release
Printed September 2006

ChISELS 1.0: Theory and User Manual

A theoretical modeler of deposition and etch processes in microsystems fabrication

Lawrence C. Musson, Rodney C. Schmidt, Pauline Ho, Steven J. Plimpton

Prepared by
Sandia National Laboratories
Albuquerque, New Mexico 87185 and Livermore, California 94550

Sandia is a multiprogram laboratory operated by Sandia Corporation,
a Lockheed Martin Company, for the United States Department of Energy's
National Nuclear Security Administration under Contract DE-AC04-94-AL85000.

Issued by Sandia National Laboratories, operated for the United States Department of Energy by Sandia Corporation.

Available to DOE and DOE contractors from
U.S. Department of Energy
Office of Scientific and Technical Information
P.O. Box 62
Oak Ridge, TN 37831

Telephone: (865) 576-8401
Facsimile: (865) 576-5728
E-Mail: reports@adonis.osti.gov
Online ordering: http://www.osti.gov/bridge

Available to the public from
U.S. Department of Commerce
National Technical Information Service
5285 Port Royal Rd.
Springfield, VA 22161

Telephone: (800) 553-6847
Facsimile: (703) 605-6900
E-Mail: orders@ntis.fedworld.gov
Online order: http://www.ntis.gov/help/ordermethods.asp?loc=7-4-0#online

SAND2006-5483
Unlimited Release
Printed September 2006

ChISELS 1.0: Theory and User Manual

A theoretical modeler of deposition and etch processes in microsystems fabrication

Lawrence C. Musson and Rodney C. Schmidt
Electrical and MicroSystem Modeling, Dept. 1437

Pauline Ho
Chemical and Biological Systems, Dept. 6215

Steven J. Plimpton
Computational Biology, Dept. 1412

Sandia National Laboratories
P.O. Box 5800
Albuquerque, NM 87185

Abstract

Chemically Induced Surface Evolution with Level-Sets—ChISELS—is a parallel code for modeling 2D and 3D material depositions and etches at feature scales on patterned wafers at low pressures. Designed for efficient use on a variety of computer architectures ranging from single-processor workstations to advanced massively parallel computers running MPI, ChISELS is a platform on which to build and improve upon previous feature-scale modeling tools while taking advantage of the most recent advances in load balancing and scalable solution algorithms. Evolving interfaces are represented using the level-set method and the evolution equations time integrated using a Semi-Lagrangian approach [1]. The computational meshes used are quad-trees (2D) and oct-trees (3D), constructed such that grid refinement is localized to regions near the surface interfaces. As the interface evolves, the mesh is dynamically reconstructed as needed for the grid to remain fine only around the interface. For parallel computation, a domain decomposition scheme with dynamic load balancing is used to distribute the computational work across processors. A ballistic transport model is employed to solve for the fluxes incident on each of the surface elements. Surface chemistry is computed by either coupling to the CHEMKIN software [2] or by providing user defined subroutines.

This report describes the theoretical underpinnings, methods, and practical use instruction of the ChISELS 1.0 computer code.

Acknowledgement

The authors would like to thank Sandia National Laboratories and the Department of Energy for supporting this work. They would also like to express thanks to Michael E. Coltrin and Robert B. Walker for many helpful discussions.

Contents

Figures

1 Introduction

The application of high-performance computing to the modeling of manufacturing processes used to produce MicroElectroMechanical System (MEMS) devices is a technological area of considerable interest to Sandia National Laboratories (SNL). In the surface micromachining (SMM) approach to the fabrication of MEMS and other microdevices, three-dimensional (3D) structures are formed by deposition and etching of thin films. ChISELS—Chemically Induced Surface Evolution with Level Sets—models from first principles the deposition and etch processes commonly used in silicon-based microdevice fabrication.

Careful control of the deposition processes, thoughtful design of the lithographic masks that pattern the wafers in dry etch and the application of a final selective release etch permits the creation of a variety of free-standing, movable parts. Deposition processes in the SUMMiT V [4] and SOI technologies developed and used by SNL include low-pressure chemical vapor deposition (LPCVD) of undoped polysilicon, P-doped polysilicon, silicon dioxide from TEOS [$Si(C_2H_5O)_4$], and Si-rich silicon nitride from $SiCl_2H_2$ and NH_3, as well as steam oxidation for the initial SiO_2 layer and the plasma deposition of SiO_2 from SiH_4 and O_2. Dry etching processes include a plasma etch of oxide and nitride using C_2F_6 and CHF_3, and of polysilicon using Cl_2, He, and/or HBr. The release etch is usually a wet etch using aqueous HF.

LPCVD processes are done in multi-wafer vertical furnaces (up to $\sim$100 wafers at once) which operate at process temperatures in the range of 500-800 C and total pressures that are usually a fraction of a Torr. The plasma processes are typically done in an unheated reactor containing only one wafer, and operate at pressures from several mTorr to fractions of a Torr.

Many of the mentioned deposition and etching processes can result in non-ideal device geometries at the feature scale. For example, CVD processes can give nearly-conformal films, but this still results in rounded corners and dimples. Step coverage can range from nearly perfectly conformal to non-conformal, and lower step coverage can result in sloped sidewalls. Under many conditions non-uniformities and irregularities in surface coverage occur. The unexpected appearance of any geometric irregularities can be particularly costly in the design, analysis, and batch fabrication cycle associated with the development of a new MEMS or other microdevice. Thus a thorough understanding of the detailed chemistry and physics which lead to these geometric variations is essential to the development of improved SMM fabrication equipment, higher yield and more reliable fabrication processes, and more useful MEMS designs.

Theoretical modeling of the detailed surface chemistry and concomitant surface evolutions during microsystems fabrication processes is a challenging problem. The viability of computational simulations for these types of problems has been demonstrated by earlier researchers and advances have been made in developing transport models, chemical mechanisms, and surface evolution modeling (*e.g.*, see [5] [6] [7]). However, currently available computer codes have not been designed to use massively parallel architectures efficiently, nor to exploit *in toto* all of the modeling advances that different researchers have made. Thus speed and robustness factors have unduly limited the size and complexity of problems that can be modeled with available tools.

The development of ChISELS is largely driven by the desire to overcome these aforementioned limitations. ChISELS 1.0 is the first released version of a parallel, 2D and fully 3D feature-scale modeler to explore the time development of material depositions and etches on patterned wafers at low pressures. ChISELS can be viewed as a platform to build and improve on previous simulation tools while taking advantage of the most recent advances in dynamic mesh refinement, load balancing, and scalable solution algorithms.

There are three inter-related aspects to modeling the overall physics of SMM process fabrication: the transport of chemical species, gas phase and surface chemistry, and the dynamic evolution of the solid surface.

In ChISELS 1.0, all gas-phase transport is assumed to occur in the free-molecular flow regime, i.e., particle-to-particle collisions are negligible. This is a good approximation for the low-pressure conditions of primary interest here and yields equations that are mathematically similar to those for the problem of radiation heat transfer. In ChISELS we adopt the ballistic transport and reaction model (BTRM) that was developed and described by Cale and coworkers [5] [8]. Details of this model and its additional assumptions are described later. A computationally significant aspect of this method is the need to calculate view-factors of the radiation-like BTRM problem in the modeling domain. For this purpose, the mathematical and numerical techniques described and implemented in Chaparral [9] are employed.

Deposition or etching occurs through the chemical reaction of and sputtering by gas phase species with bulk phase species at a surface. To model the thermodynamics and heterogeneous chemistry of these reactions ChISELS is designed to couple with the Surface Chemkin code [3] now available commercially as part of the CHEMKIN software [2]. However, it is also possible for the user to write problem-specific subroutines to model the surface chemistry. In either case, this requires the specification of a chemical reaction mechanism for each surface reaction to be modeled in the simulation.

The ability to track the evolution of a free boundary as it moves in space and time is a fundamental part of feature-scale microsystem fabrication modelers such as ChISELS. To represent this motion, a variety of both explicit and implicit surface evolution models have been developed and described in the literature.

In the explicit models, the surface is tessellated into subsurfaces. In the TopoSim3D code [10] [11], for example, a domain-spanning tetrahedral mesh discretizes the volume that surrounds the feature. Triangular surface elements subdivide the feature surface and each forms a side of a tetrahedron. Thus the volume mesh conforms to the feature surface. In other cases, only the surface itself is discretized, such as in the 3D/2D code, EVOLVE [12]. Although explicit methods can be very accurate, they often suffer from robustness difficulties associated with mesh distortion and tend to fail when large changes in topography are experienced. In particular, these types of methods often fail when proximate surfaces merge, such as can commonly occur during deposition processes in MEMS fabrication.

ChISELS uses an implicit surface-tracking approach called the level-set method. Described in Section 3, the level set approach avoids the debilitations of the explicit methods because the

mesh which is used to solve the level-set equations does not deform or conform to any surface, so distortion effects are avoided. Likewise, because a volume-defined function is evolved, merging surfaces do not create problems in the method. However, the level-set model's ability to treat geometric complexities is, in some measure, offset by accuracy issues. Thus the ability to refine the mesh in regions near the evolving surface is an important attribute of the ChISELS code. The meshes used in ChISELS are quad-trees (2D) and oct-trees (3D). The quad and oct-tree meshes are constructed such that the grid is refined only in the region of the interface. As the interface evolves, the static mesh is continually reconstructed so that the grid remains fine only around the interface. For parallel computation, the grid is distributed across the processors with each one owning a compact sub-domain. Each time the mesh is refined and coarsened, the load balance across processors is re-evaluated and redistributed so that the load remains evenly balanced regardless of changes in the grid.

2 Theoretical modeling

ChISELS 1.0 is designed to model the detailed topographical evolution of surfaces during low-pressure deposition and etching processes used in the fabrication of microscale devices. To do so requires an accurate mathematical representation of the physical processes controlling the transport of and chemical reactions between all the associated molecular species, both in the gas phase and on the surface. Figure 1 illustrates the various length-scales of interest in these processes. The largest is on the order of $10^{-1} - 10^{-2}$ m scales for a typical CVD reactor and the smallest is on the order 10^{-9} m at which individual molecules chemically react. In between is the so-called feature scale. On the order of a micron, the evolving geometry has a non-negligible effect on the transport and conversion of species. It is at this length scale that the ChISELS model is designed to operate.

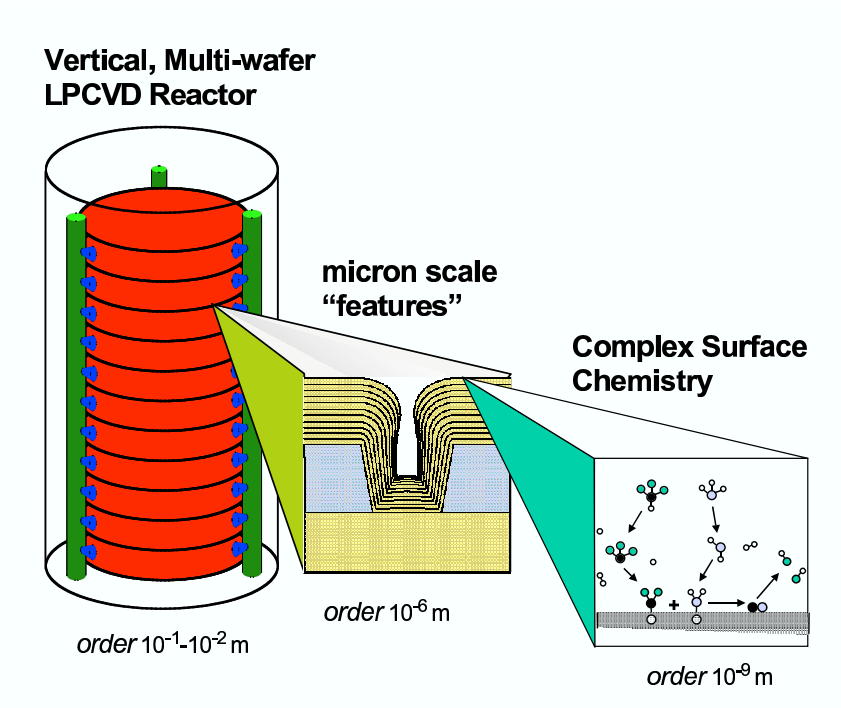

Figure 1. Illustration of length-scale variations in microsystems modeling domains.

This section begins with a description of the transport and reaction model for chemical species and surface interactions that forms the basic theoretical framework for the modeled processes. Next is described the modeling approach for treating the thermodynamics and heterogeneous chemistry that control the rates of the deposition and etching processes, albeit for cases without charged species. The current modeling approach for transport of ions in plasma-based etching and deposition processes is described next. Finally, the method used to model the evolution of the feature surface is described.

2.1 Basic Model Setup

A typical ChISELS simulation predicts the time-varying geometric change of a MEMS device feature that happens during a SMM micro-fabrication step. One example of a feature is shown in Figure 2 and is called a notch or trench, and is common in MEMS, integrated circuits and other microstructures. The notch feature will be the simple two-dimensional example used throughout this document.

To set up a calculation in ChISELS, a theoretical, or computational, domain must be defined by the user. In Chisels 1.0 the domain must be a quadrangle in two dimensions, or a hexagon in three dimensions, and it must extend entirely around the feature passing above it through the gas phase and below it through the solid phase. One two-dimensional example is shown and labeled in Figure 2.

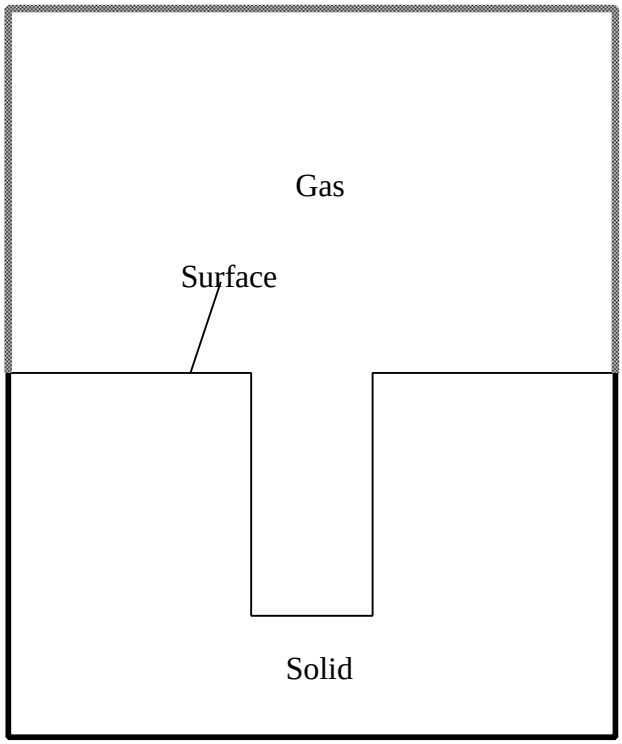

Figure 2. Theoretical domain of a ChISELS model.

In Figure 2, the thick, solid line denotes the boundary of the theoretical domain that passes through the solid beneath the feature. The thin, solid line denotes the feature surface which, in this single-material model, is a phase boundary dividing solid from gas. The thick, shaded line is the boundary of the theoretical domain that passes through the gas phase above the feature surface.

In a process, gas reactants diffuse through the shaded boundary. When these reactants strike the feature surface, they can stick and re-emit or they can react and emit products while simultaneously depositing material or etching it away. The result of this reaction is to cause the gas-solid boundary to be set in motion. If a net material deposition is the result, the feature surface will invade into the

gas subdomain, and vice versa if a net material etch is the result.

What follows in the ensuing sections is a description of the theoretical models that are solved in the user-defined domain shown in Figure 2.

2.2 Ballistic Transport and Reaction Model

In ChISELS, the ballistic transport and reaction model (BTRM) as developed and described by Cale and coworkers (see [5] [8]) is adopted. This model provides a good model of low-pressure deposition and etch processes such as physical vapor deposition (PVD), low-pressure chemical vapor deposition (LPCVD), plasma-enhanced chemical vapor deposition (PECVD), and reactive ion etching (RIE). These processes are important and have long been used in the manufacture of MEMS and other silicon-based microsystems. The explanation provided here is an abbreviated description of the model extracted from the aforementioned references.

The BTRM model is applicable when the following assumptions hold:

1. The frequency of particle-particle collisions among gas phase species is negligible compared to collisions between gas-phase species and surfaces. This condition is characterized by a high Knudsen number—the ratio of the mean free path of a particle to the appropriate length scale.

2. Topographical changes due to surface growth rates evolve slowly relative to the redistribution of the local fluxes and reaction rates.

3. The deposition/etch rate is governed by heterogeneous reaction mechanisms and depends on the local species fluxes.

4. Gas-phase species arrive at the surface from the source volume with well defined, species-specific flux distributions.

For LPCVD models, we also make two additional assumptions: species re-emit from surfaces with a diffuse Maxwellian velocity distribution, and reaction rates do not depend on the incident angle or collision history of the impinging molecules. Figure 3 shows a schematic of the 2D modeling domain of an LPCVD process comprised of reactive neutrals.

As in most computer-based models, the theoretical domain, or what can now be called the computational domain, must be divided into discrete subdomains which assemble to produce the whole. Only the transport in the gas phase and reactions on the surface are germane to the BTRM model, so only the gas-phase portion of Figure 2 need be considered.

As shown in Figure 3, the gas-phase boundary and the feature surface are subdivided into linear elements. The method by which it is done is described in the next chapter. In low-pressure processes, the transport in the gas phase adjacent to the feature surface may be approximated by

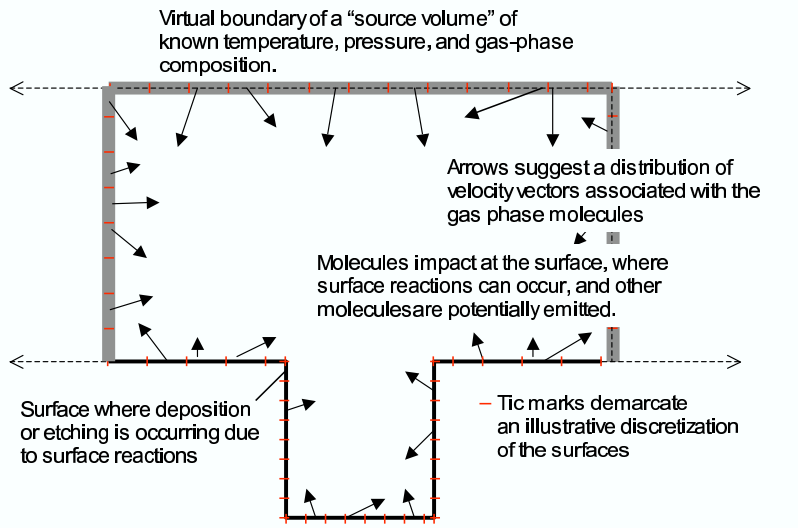

Figure 3. Schematic drawing of the Ballistic Transport and Reaction Model

straight-line, or ballistic, motion. The mathematical problem of modeling such ballistic transport and reaction is analogous to enclosure radiation, viz.

$$\begin{pmatrix} \mathbf{F} \\ \mathbf{F_0^0} \end{pmatrix} = \begin{bmatrix} \mathbf{G} & \mathbf{G^0} \\ \mathbf{G_0} & \mathbf{G_0^0} \end{bmatrix} \begin{pmatrix} \mathbf{F}+\mathbf{R} \\ \mathbf{F_0}+\mathbf{R^0} \end{pmatrix} \tag{1}$$

where $\mathbf{F}$ is the vector of fluxes of each species to the feature surface, $\mathbf{F_0^0}$ is the vector of fluxes to the hypothetical gas surfaces, $\mathbf{G}$ is a matrix of view factors between surface elements on the feature surface, $\mathbf{G^0}$ is the matrix of view factors between surface elements on the feature surface and feature elements on the hypothetical gas boundary, $\mathbf{G_0}$ is the complement to $\mathbf{G^0}$ [9], $\mathbf{G_0^0}$ is the matrix of view factors between surface elements on the hypothetical gas boundary, and $\mathbf{R}$ and $\mathbf{R^0}$ are the reaction rates on the feature surface and the hypothetical gas boundary surface elements respectively.

Many of the terms in Equation (1) can be condensed out. Because gas surfaces are hypothetical, material fluxes to them from other hypothetical surfaces or from the feature surface simply pass through into the greater volume of the reactor. The values of these fluxes and their composition are immaterial to the computation and may be disregarded. $\mathbf{F_0}$ is a flux from the reactor through the gas surface into the theoretical domain. These fluxes can be calculated from other theories to be described later and are thus known. $\mathbf{R^0}$ must be zero. Therefore, Equation (1) can be rewritten, now with component indices, as

$$F_{ik} = F_{ik}^0 + G_{ij}\left(F_{jk} + R_{jk}\right) \tag{2}$$

where F_{ik} is the flux of species k to surface i, $F_{ik}^0 = G_{ij}^0 F_{jk}^0$ is the direct flux from the reactor, G_{ij} is the view factor between surface i and j, F_{jk} is the flux of species k to surface j, R_{jk} is the reaction rate of species k on surface j. By Einstein's notation, repeated indices in the products imply summation.

Equation (2) defines a quasi-equilibrium state where the transport of species to and from surfaces in an enclosure is exactly balanced by the surface reaction rates. To solve for the species fluxes on each solid surface, the geometric view factors, the fluxes from the reactor, and the reaction rates for each species on all surfaces must be known.

View factors are a function of the discretized surface geometry of the enclosure and can be computed independently of the species fluxes and the reaction rates. Because the topography changes due to the deposition or etching process, the view factors also change. So the view factors must be continually recomputed.

The view factor between two finite surfaces i and j is given by

$$G_{ij} = \frac{1}{A_i} \int_{A_i} \int_{A_j} \frac{cos\theta_i cos\theta_j}{\pi r^2} \delta_{ij} dA_j dA_i \tag{3}$$

where δ_{ij} is determined by the visibility of dA_j to dA_i, and is equal to one if dA_j is visible to dA_i or is equal to zero otherwise, cf. Figure 4.

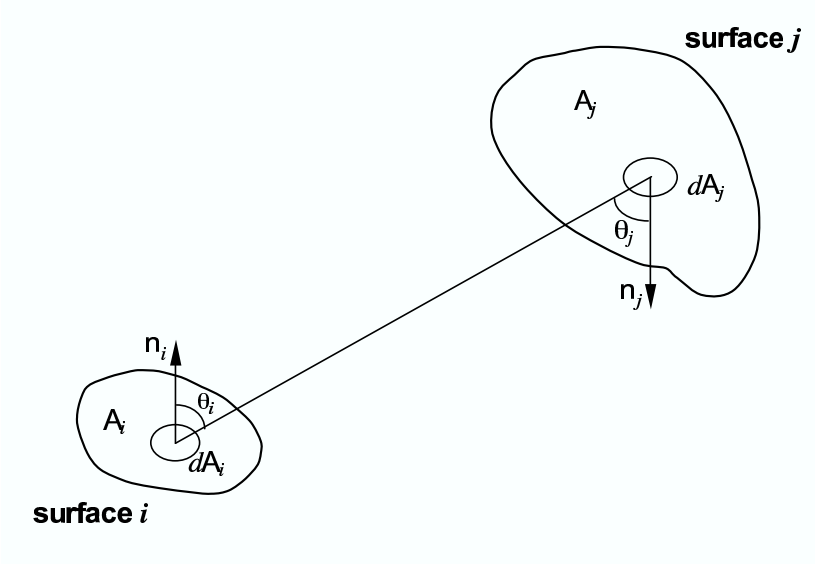

Figure 4. Geometry and nomenclature for calculating view factors between finite areas

In ChISELS, view-factors are computed each time step by evaluating the surface integrals defined in Equation (3), by any one of the methods which are briefly discussed in Section 3.1.

Given the thermodynamic state and species concentrations in the reactor, the source flux density, F_{ik}^0, is calculated from kinetic gas theory [13] from

$$F_{ik}^0 = \frac{\gamma_k P}{RT} \sqrt{\frac{RT}{2\pi W_k}} \tag{4}$$

where γ_k is the mole fraction of species k, P and T are the thermodynamic pressure and temperature, R is the universal gas constant, and W_k is the molecular weight of species k. Equation (4) can be

derived assuming the gas obeys ideal state law where the molecules have a Maxwellian velocity distribution.

The final ingredient needed for Equation (2) to be solved is the complete set of surface reaction rates, R_{jk}; these rates are non-linear functions of the incident fluxes F_{ik}. Reaction rate chemistry, and the models used to represent these processes in ChISELS are described separately in the next sub-section.

2.3 Reaction Rate Chemistry

Heterogeneous chemical reactions at the interface between a solid surface and an adjacent gas are the physical basis for the deposition and etching processes modeled by ChISELS. Specifically, to solve Equation (2), the reaction rate R_{jk} for each species k on each surface j must be calculated. To model these reactions, ChISELS couples to the CHEMKIN software [2]. However, it is also possible for the user to write problem-specific methods to model the surface chemistry.

In this section an abbreviated discussion of the mathematical formalism used to describe the surface kinetics of these processes is provided. This will define the mathematical rules for keeping track of surface species concentrations, the conservation of mass and surface sites, mass-action kinetics, and deposition or etching rates. Here we adopt much of the formalism developed for the CHEMKIN software package. The following discussion is adapted from the documentation and manuals for the CHEMKIN software, e.g. see [3] [2]. The reader is directed to those documents for a more detailed discussion.

2.3.1 Types of Species

In a ChISELS model, there are three types of species: gas-phase, surface, and bulk. The first is a species in the gas phase above the surface, which will be denoted in a reaction by (g). A surface species, denoted by (s), is defined to be the chemical species on the top-most layer of the solid, i.e., at the solid-gas interface. Each surface species occupies one or more sites whose total number is assumed to be conserved. Any species in the solid below the surface layer is defined to be a bulk species and is denoted by (b). Note that although the (g), (s) and (b) naming conventions are used in this discussion to indicate phase, the software does not require that the species be named this way.

More than one type of site can be defined on the surface. For each site-type, n, the site density Γ_n (e.g. $moles/cm^2$) must be specified as part of the reaction mechanism. Furthermore, one may define a species that only resides on a certain type of site. For example, the thermodynamic properties of a hydrogen atom on a site-type A might be different from a hydrogen on a site-type B, and they could be specified as different species even though their elemental composition is the same. The population of different species occupying a given site-type is specified by site fractions, $Z_k(n)$, whose sum on a given site-type is 1.

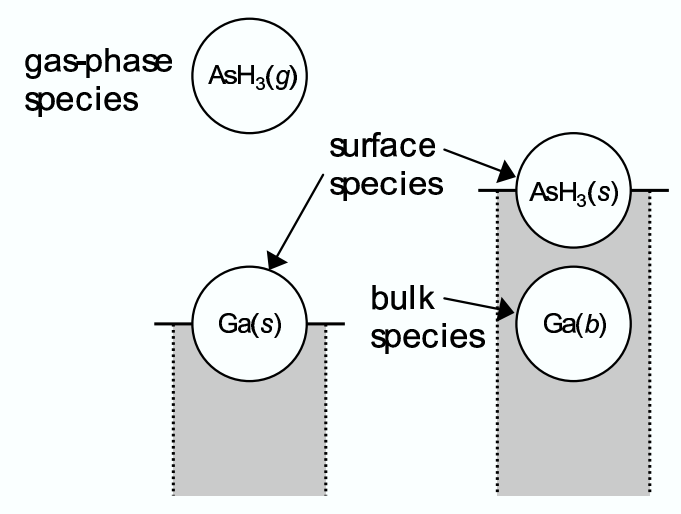

Figure 5. Illustration of the conceptual picture used for a simple adsorption reaction (adapted from [3])

For simplicity, the discussions and equations that follow will neglect the annotations designating the site-type n. That is, there is only one type of site in the mechanism. However, ChISELS through CHEMKIN is fully capable of treating multiple site-types.

In the bulk there can be different types of bulk species. Typically, there is only one species. ChISELS does not maintain a history of the bulk composition—only the phase boundary between solid and gas.

2.3.2 Representation of Surface Reactions

In ChISELS, heterogeneous chemistry contains reactions between species in the gas and solid phases plus the interface between them. As illustrated in Figure 5, a chemical species on the top layer of the solid, i.e., a surface species, occupies a site. For example, an arsine molecule adsorbed on a surface could occupy a site, and might be denoted $AsH_3(s)$. Another example might be a bare gallium atom, $Ga(s)$, on top of a gallium arsenide crystal. Now consider the case if another species, say a gas-phase AsH_3, lands on top of the $Ga(s)$. The gallium atom that was at the surface is covered up, so it is no longer a surface species but has become a bulk species. Because the adsorbed AsH_3 now occupies the top-most layer at this site, it is now a surface species, viz. $AsH_3(s)$. This adsorption reaction is represented by the following stoichiometric relation,

$$AsH_3(g) + Ga(s) \Rightarrow AsH_3(s) + Ga(b). \tag{5}$$

The reverse of this adsorption reaction is the desorption reaction, viz.

$$AsH_3(s) + Ga(b) \Rightarrow AsH_3(g) + Ga(s). \tag{6}$$

$Ga(b)$ is included as a reactant in order to achieve site and elemental balance. In the CHEMKIN manuals [2] the formalism described in reactions (5) and (6) is called the “Atomic Site Formalism.”

An alternative but equally viable formalism therein described is called the "Open Site Formalism," but is not discussed here.

The set of I surface reactions involving K chemical species is represented in the following general form for a reversible reaction

$$\sum_{k=1}^{K} \upsilon_{ki}^{'} \chi_k \Leftrightarrow \sum_{k=1}^{K} \upsilon_{ki}^{''} \chi_k \qquad (i = 1, 2, ..., I) \tag{7}$$

where $\upsilon_{ki}^{'}$ and $\upsilon_{ki}^{''}$ are the forward and reverse stoichiometric coefficients of the reactant and product species in the elementary reactions and χ_k is the chemical symbol for the k^{th} species.

2.3.3 Species Reaction Rates

The net reaction rate R_k (called the species production rate $\dot{S}_k$ in the CHEMKIN manuals [2] [3]) for each of the K species is the sum of the rates of reaction for all reactions containing the k^{th} species:

$$R_k = \sum_{i=1}^{I} \upsilon_{ki} q_i \qquad (k = 1, 2, ..., K) \tag{8}$$

where υ_{ki} is defined to be

$$\upsilon_{ki} = (\upsilon_{ki}^{''} - \upsilon_{ki}^{'}) \tag{9}$$

and the rate-of-progress variable q_i for the i^{th} reaction is given by the difference between the forward rates and the reverse rates:

$$q_i = k_{f_i} \prod_{k=1}^{K} [X_k]^{\upsilon_{ki}^{'}} - k_{r_i} \prod_{k=1}^{K} [X_k]^{\upsilon_{ki}^{''}} \tag{10}$$

where $[X_k]$ is the molar concentration of species k.

The forward rate constants k_{f_i} for the I reactions are often assumed to have the following type of Arrhenius temperature dependence:

$$k_{f_i} = A_i T^{\beta_i} exp\left(\frac{-E_i}{R_c T}\right) \tag{11}$$

where R_c denotes the universal gas constant in activation energy units, and where the pre-exponential factor A_i, the temperature exponent β_i, and the activation energy E_i must be specified. In CHEMKIN, the default units for R_c and E_i are $cal/mole$. However, a variety of modifications and alternative formulations for parameterizing the rate constants are possible; these are described in the CHEMKIN manuals [2].

For reversible reactions, the reverse rate constants k_{r_i} are related to the forward rate constants k_{f_i} through the equilibrium constants K_{c_i} as

$$k_{r_i} = \frac{k_{f_i}}{K_{c_i}}. \tag{12}$$

2.3.4 Surface-Reaction Rate Dependence on Local Species Fluxes

Surface reaction rates are dependent upon the rate at which gas-phase species arrive at a given surface location. This produces a non-linear coupling between the surface-reaction rates and the species fluxes throughout the feature. The model used in ChISELS to address this coupling is called the ballistic transport and reaction model (BTRM) and is similar to other approaches [12], [11]. In order to compute species reaction rates, the molar flux densities computed in the BTRM model must be converted to the state variables used in equilibrium chemistry.

Part 1: Computing the near-surface gas-phase concentrations For chemistry consisting only of neutrals, it is assumed that the concentration of each gas-phase species immediately adjacent to each location on the surface can be calculated as a function of the temperature and the magnitudes of the net fluxes of each species to that surface.

The flux of any species k can be written as the product of a species density and the average species velocity, i.e.

$$F_k = \rho_k \bar{V_k}. \tag{13}$$

From kinetic gas theory, the mean molecular velocity in an ideal gas is

$$\bar{V_k} = \sqrt{\frac{RT}{2\pi W_k}} \tag{14}$$

Equation (14) and Equation (13) yields for ρ_k

$$\rho_k = \frac{F_k}{\sqrt{\frac{RT}{2\pi W_k}}} = F_k \sqrt{\frac{2\pi W_k}{RT}}. \tag{15}$$

To convert density to species concentration, multiply by the molecular weight to produce the relationship

$$[\chi_k] = F_k W_k \sqrt{\frac{2\pi W_k}{RT}} \tag{16}$$

It is also often useful to compute the species partial pressures. Solve for partial pressure using the ideal gas law and Equation (15):

$$P_k = \rho_k RT = F_k \sqrt{2\pi W_k RT}. \tag{17}$$

Part 2: Computing surface-species site fractions Based on the near-surface species concentrations, surface-species site fractions are calculated that are consistent with these conditions under the assumption that the chemical reactions proceed at a steady rate. In consequence, the time-rate of change of surface site fractions is zero. Here is described how, under these conditions, the rate equations are used to compute the desired site fractions.

For convenience in the equations that follow, the definitions are generalized of the site density and the site fractions of the k^{th} species so that they have meaning for the bulk, gas-phase and surface species. To this end,

$$\Gamma_k(g) = \Gamma_k(b) = 1 \qquad \textit{and} \qquad \Gamma_k(s) = \Gamma \tag{18}$$

and

$$Z_k = [\chi_k]/\Gamma_k \tag{19}$$

where the total site density Γ is a constant that must be provided with the reaction mechanism specifications.

With these definitions, all species concentrations, regardless of phase, can be expressed as

$$[\chi_k] = \Gamma_k Z_k. \tag{20}$$

The concentration units in the bulk or gas phase are $moles/cm^3$, but on a surface, the units are $moles/cm^2$.

The total number of species K, is equal to the sum of the number of gas-phase species K_g, the number of surface species K_s, and the number of bulk species K_b.

$$K = K_g + K_s + K_b \tag{21}$$

The time-rate of change of surface species site fractions is found by combining Equations (8) and (10) with the above definitions to yield

$$R_k(s) = \Gamma \frac{d[Z_k(s)]}{dt} = \sum_{i=1}^{I} \upsilon_{ki} \left(k_{f_i} \prod_{k=1}^{K} (\Gamma_k Z_k)^{\upsilon_{ki}^{'}} - k_{r_i} \prod_{k=1}^{K} (\Gamma_k Z_k)^{\upsilon_{ki}^{''}} \right). \tag{22}$$

In steady operation, $\frac{d[Z_k(s)]}{dt} = 0$ so that the following equations result from which the K_s values of the surface-species site fractions are solved

$$0 = \sum_{i=1}^{I} \upsilon_{ki} \left(k_{f_i} \prod_{k=1}^{K} (\Gamma_k Z_k)^{\upsilon_{ki}^{'}} - k_{r_i} \prod_{k=1}^{K} (\Gamma_k Z_k)^{\upsilon_{ki}^{''}} \right) \tag{23}$$

and

$$\sum_{k=1}^{K_s} Z_k = 1.0 \tag{24}$$

Example

This simple example system consists of three gas phase species, $H_2(g)$, $SiH_2(g)$ and $SiH_4(g)$, two surface species, $Si(s)$ and $SiH(s)$, and one bulk species, $Si(b)$; therefore K_g = 3, K_s = 2, K_b = 1, and K = 6. The following three irreversible surface reactions are specified in the reaction mechanism:

$$SiH_4(g) + 2\ Si(s) \Rightarrow 2\ SiH(s) + Si(b) + H_2(g)$$

$$2\ SiH(s) \Rightarrow 2\ Si(s) + H_2(g)$$

$$SiH_2(g) \Rightarrow Si(b) + H_2(g)$$

For this example we can apply Equation (23) (for either the $Si(s)$ or the $SiH(s)$) to get

$$0 = 2k_{f_1}[SiH_4](\Gamma Z_{Si(s)})^2 - 2k_{f_2}(\Gamma Z_{SiH(s)})^2 \tag{25}$$

and use Equation (24) to write

$$Z_{Si(s)} + Z_{SiH(s)} = 1.0. \tag{26}$$

Given the expressions for the rate constants k_{f_1} and k_{f_2}, and values for the site density Γ and the near-surface gas-phase concentration $[SiH_4]$, these two equations can be solved for $Z_{Si(s)}$ and $Z_{SiH(s)}$.

2.4 Reactions for Plasma Processes

The technologies used for MEMS fabrication include several plasma processes for deposition and etching. Plasma processes are also used to alter surface morphology, sputter material, or enhance chemical reactions. One advantage of plasma over thermal processes is that they allow the use of substantially lower substrate temperatures. More importantly, for etching they allow non-isotropic or directional etching of the surface. This involves accelerating the positive ions into the substrate by applying an electrical bias, which causes etching reactions to occur preferentially at the bottom of a feature rather than at the sides. This, in turn, allows the fabrication of MEMS devices with high-aspect-ratio geometries. In such cases, the directed energy of ions encountering a surface will be significantly greater than the ion temperature in the plasma gas.

The CHEMKIN Software includes a reactor model for zero-dimensional plasma simulations, and ChISELS adopts the formalism used there for describing plasma systems. The most important aspects of this formalism are briefly described here. More details and usage options can be found in the CHEMKIN Manuals [2]. The plasma formalism consists primarily of three additional components to non-plasma formalism:

1. The use of separate temperatures for neutrals, electrons and ions,

2. The treatment of electron impact reactions in the gas-phase, and

3. The treatment of ion-enhanced surface reactions.

This last component is the most important for ChISELS, so it is discussed in the most detail below.

Many of the plasmas used in materials processing are non-equilibrium, or low temperature, plasmas, where the neutrals, ions and electrons are not in thermal equilibrium. Generally, the electrons have much higher energies than the ions, which in turn have higher energies than the neutrals. Separate temperatures are therefore defined and tracked for these classes of species. By default, reaction rates depend on the temperature of the neutrals, but optional keywords can be used in the mechanism description to alter this.

This multi-temperature description requires care when converting between partial pressures, mole fractions, concentrations and molecular fluxes. For example, the simple expression for the ideal gas law given in Equation (17) is replaced by

$$P_k = \sum_{k=1}^{K} [\chi_k] R T_k \tag{27}$$

where the partial pressure of each species is calculated with the relevant temperature, according to the species type. The electron temperature is generally much higher than the others, so even though the electron density tends to be relatively low, it can make a significant contribution to the total pressure. The other equations used for interconverting these quantities, Equations (14)-(16), also need to be used with the appropriate temperature. Note, however, that in a plasma system with an applied bias, the velocity/flux of the ions toward a biased surface will be obtained from the separately determined ion energy and the Bohm Condition described below, rather than by use of the ion temperature in these equations.

Electron impact reactions are generally part of the gas-phase reaction mechanism, and depend on the electron temperature rather than that of the neutral species. These reactions are not explicitly used by ChISELS, but rather are part of the reactor-scale simulations that would provide the input chemical compositions for ChISELS. Electron energy distributions often deviate from Maxwellian, but approximating them as thermal distributions is generally acceptable in view of the uncertainties in the electron impact cross-sections and chemical reaction rates.

2.4.1 Ion-Surface Reactions

The CHEMKIN formulation for ion-enhanced surface reactions [2] includes: (1) a special rate expression for cases where reaction yields depend on ion energy, and (2) a modification of the ion flux to the surface. In this treatment, electrons are assumed to be much more mobile than the ions such that electron transport to the surface does not affect surface neutralization rates.

Ion Energy Dependent Yields. In modeling plasma systems, it is sometimes necessary to include reactions where the energy of the incident ion determines not only the reaction rate, but also the number of product species formed. The CHEMKIN formalism for ion-enhanced etching

reactions allows for such a variable stoichiometry. The number of species etched from the surface per incident ion is described using a yield enhancement factor that depends on the incident ion energy.

An example of a reaction using the ion-enhanced yield option in the form used by CHEMKIN is:

$$E + Ar^+ + \#SiCl_2(S) + \#Si(B) \Rightarrow Ar + \#SiCl_2 + \#Si(S), \tag{28}$$

where the special character # is the energy-dependent multiplicative factor for the stoichiometric coefficient. In this case, the yield of this reaction is per incident Ar^+ ion. The positive argon ion Ar^+ hits a silicon surface and is neutralized by reaction with a gas-phase electron (E). The surface is covered by chlorinated surface sites and each ion impact consumes a variable number of the $SiCl_2(S)$ surface species. For each surface species $SiCl_2(S)$ destroyed, the example reaction consumes a bulk silicon species $Si(B)$ and produces a $SiCl_2$ gas phase species plus an open surface silicon species $Si(S)$. Note that the sub-reaction consisting of every species preceded by the # sign balances in mass, elements, charge, and number of surface sites.

The yield (ψ) depends upon the energy of the ion with the following functional form:

$$\psi(E_{ion}) = h_{yield} \times max\left[0, (E_{ion}^{t_i} - E_{yield,0}^{t_i})^{u_i}\right], \tag{29}$$

where $E_{yield,0}$ represents a threshold energy, and the energy expressions can be raised to a specified power in two different ways through the use of the parameters t_i and u_i. Based on experimental observations, a value of one-half for the t_i parameter and a value of one for the u_i parameter are generally used, but the functional form accommodates more variability. These ion-energy dependent yields can only be used for irreversible reactions involving a single positive ion species.

Bohm Condition for Ion Fluxes The plasma reactor model within CHEMKIN is a zero dimensional model, so it does not explicitly treat the effects of the plasma sheath that forms near surfaces. Instead, the effects of the sheath are treated by applying the Bohm Criterion. This treatment is currently implemented in ChISELS, although more detailed sheath models could be added as needed.

There are two parts to the Bohm Condition: the Bohm limitation to ion fluxes, and the correction in the presence of negative ions. For very low-pressure plasmas in the absence of negative ions, it is reasonable to constrain the ion flux to a surface according to the Bohm condition. This condition maintains that the maximum net flux of a particular ion to a surface is equal to the product of the ion density and the Bohm velocity, which is defined as

$$U_{Bohm} = \left(\frac{RT_e}{W_i}\right)^{1/2} \tag{30}$$

where T_e is the electron temperature, and W_i is the molecular weight of the positive ion. The user is also allowed to input a correction factor ξ for the Bohm condition which leads to the following

expression:

$$IonFlux = \xi c_i U_{Bohm} = \xi c_i \left(\frac{RT_e}{W_i} \right)^{1/2} \tag{31}$$

where c_i is the concentration or number density of the ion.

In the presence of negative ions, there is an additional correction factor. The expression for the ion speed at the sheath is

$$U_{Bohm,NegIons} = \left(\frac{RT_e}{W_i} \right)^{1/2} \left[\frac{(c_i + c_e)}{(c_i T_e + c_e T_i)} \right]^{1/2} \tag{32}$$

where c_e is the electron molar concentration and c_i is the sum of the ion molar concentrations. In the CHEMKIN plasma reactor model, there are two approaches to specifying the Bohm limit. The difference between the two approaches arises when an ion participates in more than one surface reaction subject to the Bohm criterion. In one case, the net ion flux to the surface will be automatically scaled to the Bohm-limiting flux, modified for electronegative gases and the user-defined correction factor. In the other case, each reaction will be subject to the Bohm limit independently, and the user must make sure that the reaction coefficients ξ add up to the desired overall correction factor for all the reactions involving a particular ion. In the 0D plasma reactor model, the overall correction factor is often used to account for spatial variations in ion density or transport limitations in the reactor being modeled, and the plasma reaction mechanisms are generally developed using this automatic scaling approach. The automatic scaling approach was thus implemented in ChISELS.

Angular Dependence of Ion-enhanced Surface Reactions The probability of reaction, neutralization or reflection of an ion at the surface can be specified within the existing CHEMKIN formulation. At the feature-scale, however, the effects of the directionality of the ions also need to be included.

In the current version of ChISELS, the incoming ions are traveling substantially normal to the hypothetical boundary for the source volume with a velocity determined by the Bohm criterion. A small spreading angle can be specified by a user input parameter to account for deviations from perfect uniform directionality. For ChISELS 1.0, the ions are assumed to neutralize with unit probability upon impact with the surface. Cases in which positive ions only partially neutralize on impact with a surface must await future versions of ChISELS that explicitly treat the effects of electromagnetic fields.

The angle at which the incoming ions hit the surface (here denoted θ) can also affect the rates of the ion-surface reactions. Although by default this effect is not modeled, several user-activated options are available which address this issue by the definition of an angle dependence curve. For example, a user might want to use the normal component of the ion energy to calculate the yield of an ion-assisted surface reaction. This option, activated by the "cosine_yield" input command (to be explained later) is quite reasonable for a reaction where the energy of the ion collision with the

surface enhances the etching chemistry. A closer examination of the literature, however, suggested that a different angular dependence might be more appropriate for some reactions that are closer to a physical sputtering process. For example, Chapman [14] shows a case where the sputtering yield has a maximum roughly 45 degrees from the surface normal, with the details of the shape of the curve and the location of the maximum varying with material and ion energy. In ChISELS 1.0 four types of curves are available to model different types of possible angular dependencies. They are illustrated in Figure 6. The first three correspond to the following functional aproximations for the yield factor $Y_{factor}(\theta)$;

Cosine:

$$Y_{factor}(\theta) = cos(\theta) \tag{33}$$

Polynomial:

$$Y_{factor}(\theta) = A + B\theta + C\theta^2 + D\theta^3 \tag{34}$$

Trigonometric:

$$Y_{factor}(\theta) = A\left[Bsin(C\theta - \frac{\pi}{2}) + Dcos(E\theta)\right] \tag{35}$$

The fourth option is a cubic spline representation that cannot be written as a single equation. It is defined by three user-input conditions: the extend of the initial constant region, the location of the peak, and the magnitude of the peak, as illustrated in Figure 6d.

How these optional yield factor functions are used and specified is described in Section 4.2.

The neutral species that are produced when the ions are neutralized, along with gas-phase species created by ion-enhanced surface reactions, are assumed to thermalize with the surface. They are assumed to be emitted with an energy distribution representative of the temperature that was input by the user and with a cosine angular dependence.

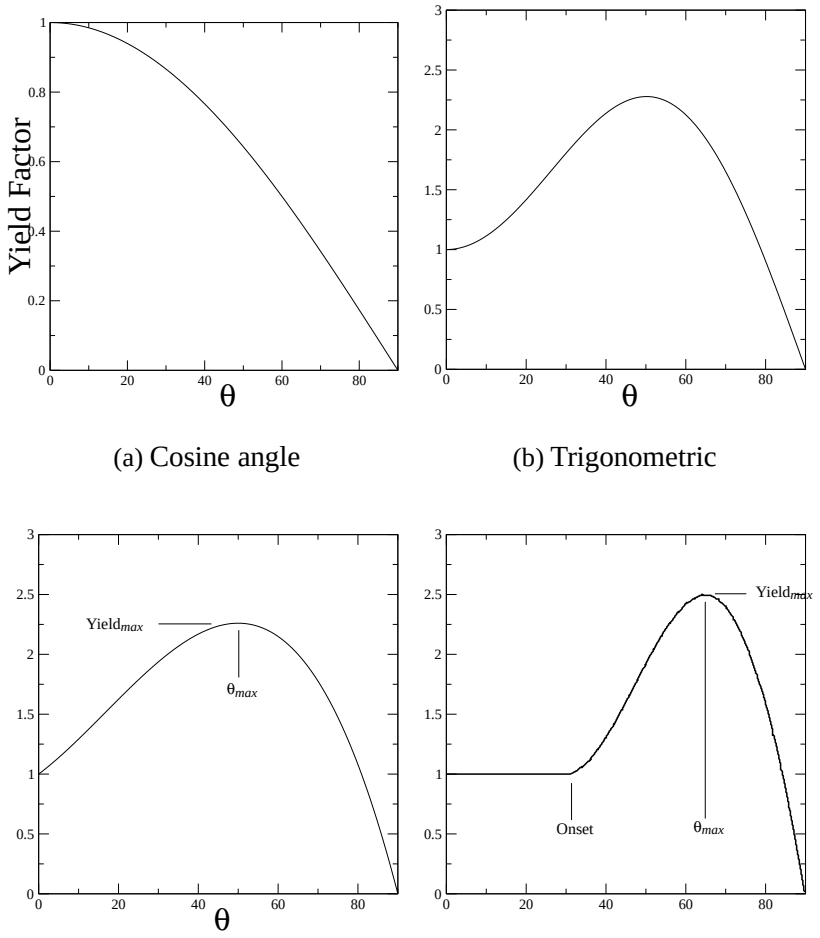

(a) Cosine angle (b) Trigonometric

(c) Polynomial (d) Spline

Figure 6. Angle of incidence functions on ion yield. θ is angle from perpendicular of ion impact.

2.5 Level-Set Method

The problem of representing accurately the temporal evolution of a moving interface is a challenging one that appears in many problems of physics. A variety of both explicit and implicit methods for modeling interface evolution have been developed over the years. Explicit, or so-called Lagrangian methods represent the interface by a collection of discrete points or material filaments which share material coordinates with the surface, and which are advected with the velocity of the surface. These methods can be classified as either front-tracking methods [15]—where the surface is represented by contiguous material filaments, or marker-point methods [7]—where the surface is represented by a collection of points. Implicit, or so-called Eulerian methods, such as the volume-of-fluid [16] and the level-set method [7], define the interface implicitly by a scalar quantity from which the interface can be deduced locally on a stationary grid. Each of these approaches has particular advantages and disadvantages, and the problem of interface tracking continues to be an area of active research [17].

For problems with large topographical changes, such as may occur in the feature length-scale modeling of MEMS and microelectronic fabrication processes, the level-set method has distinct advantages. Of particular note is that the merging or pinching-off of colliding surfaces is handled naturally without *ad hoc* rules or the necessity of user interaction. It is primarily for this reason that the level-set method was chosen for use in ChISELS.

In the level-set method, a domain-spanning function, ϕ, is defined. The zero-value contour of this function, or level set, conforms to the feature surface. In this case, the theoretical domain is the full box in Figure 2 including both solid and gas domains. The level-set function is evolved by solving the following scalar partial-differential equation,

$$\frac{\partial \phi}{\partial t} + \mathbf{v} \cdot \nabla \phi = 0 \tag{36}$$

over the volume and integrating through time.

To solve Equation (36) the velocity field $\mathbf{v}$, the so-called extension velocity, must be specified. In fluid flow problems, the extension velocity field matches the fluid velocity found by solving momentum and continuity equations. In the etching and deposition problems being modeled by ChISELS, a convenient, domain-spanning velocity field does not exist. Instead, the local deposition or etch rate at each point on the surface is known, and this implicitly defines an effective normal surface velocity. An extension velocity field must be calculated from the interface velocity such that the level set of ϕ evolves in such a way that it accurately represents the evolution of the feature surface. In ChISELS, the extension velocity is set at discrete locations equal to the velocity of the nearest location of the feature surface. These discrete locations are the same as the nodal locations of a mesh whose construction is described in a later section.

When the level-set method is employed, errors can accrue in the computed shapes and locations of the evolving surface from two sources. First, when the signed distance function is represented by a finite set of basis functions, as it must be in computer implementations of the method, insufficient resolution from the use of too few basis functions of the signed distance function can result in an

inaccurate resolution of the surface, particularly in regions of high curvature. Likewise, if the extension velocity is not accurately chosen, the interface will not evolve faithfully to that which the physics demands. However, both of these sources of error can be mitigated through increased mesh resolution, a topic discussed later in Section 3.3.

3 Modeling Strategies

In this section, the methods used by ChISELS to solve the theoretical models laid out in Section 2 are each discussed in turn.

3.1 View-Factor Calculation

The BTRM model used in ChISELS requires the calculation of viewfactors between each surface element on the discretized surface. In ChISELS 1.0, these viewfactors are calculated by calling routines in Chaparral [9], a Sandia developed library package originally written for solving large three-dimensional enclosure radiation heat transfer problems. Like ChISELS 1.0, the current version of Chaparral is also designed for use on parallel machines using the standard MPI library.

Chaparral includes a variety of methods to calculate viewfactors, including traditional line integration, double area integration, and hemi-cube methods. The hemi-cube method is particularly advantageous for complex 3D geometries with obstructed views, such as may occur in a ChISELS calculation. Additional details about the Chaparral code can be found in ref. [9].

3.1.1 Modification for Preferred-Direction Transport

Many plasma etching processes involve the acceleration of positive ions into the substrate by applying an electrical bias. In such cases, ChISELS 1.0 assumes that the ion transport is uniformly directional (although possibly having a small user defined spreading angle) and that reaction rates at the surface are essentially instantaneous. This means that all ions reaching a given surface originate from the source surface, travel in a straight line path, and have a 100 percent probability of reacting. Thus, for positive ion transport, Equation (2) is greatly simplified due to the fact that $F_{jk} = -R_{jk}$. Under these conditions the flux of any positive ion species k to surface i from source element j can be written as

$$F_{ik} = F^0_{ik} = G^{d0}_{ij} F^{d0}_{jk} \tag{37}$$

where the superscript $d0$ denotes that the view factor and flux have a preferred direction. Because of this directionality, the values of G^{d0}_{ij} must be specially calculated.

Figure 7 illustrates the geometric considerations that must be accounted for in calculating the values of G^{d0}_{ij}. In the situation shown nothing obstructs the direct line of sight between a surface element i and the associated window in the source plane from which ions can directly reach this element. Two angles are defined; the spreading angle ϕ; a small positive value defined by the user, and the orientation angle θ_i; defined as the angle formed between the surface element normal vector and the source plane normal vector. Given these two angles, and knowing the geometric coordinates of the surface element and the source plane (as illustrated), the location and dimensions of the ion flux "window" in the source plane can be found as shown.

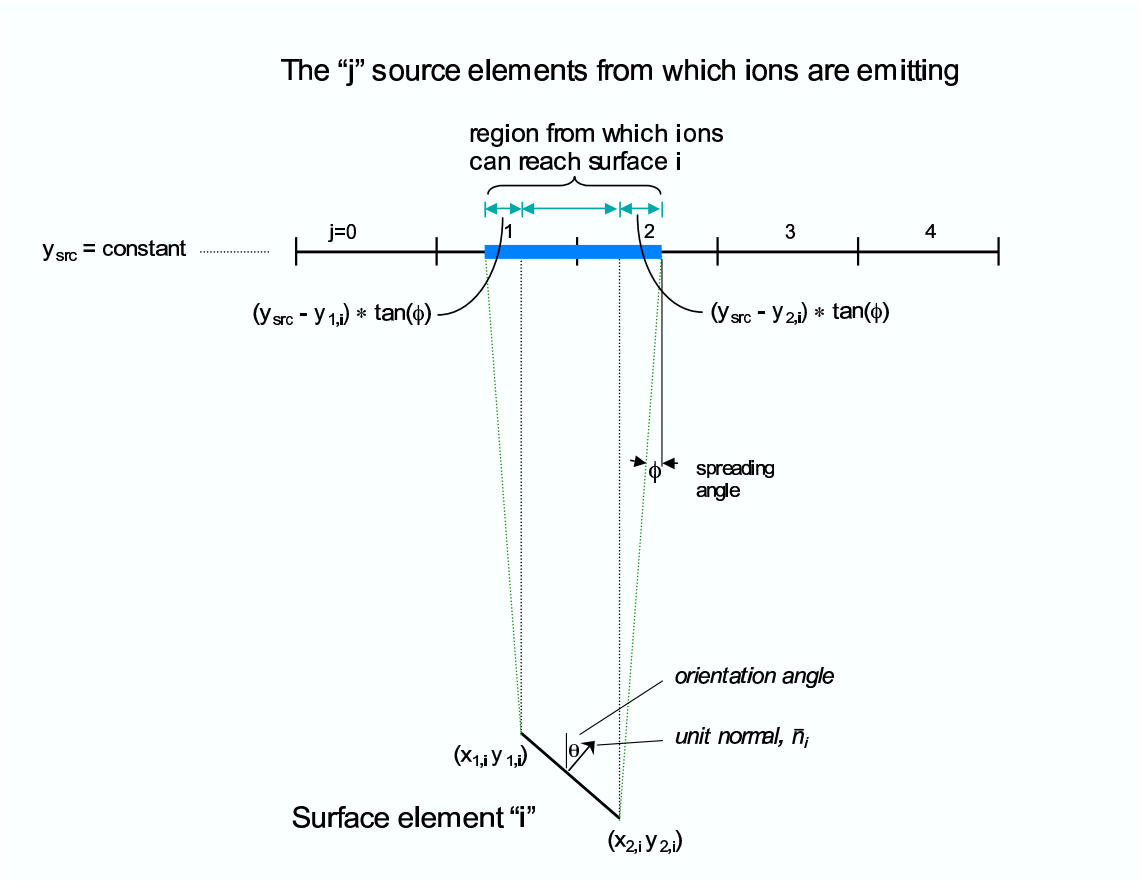

Figure 7. Illustration of geometric considerations needed to calculate directional viewfactors for ion transport

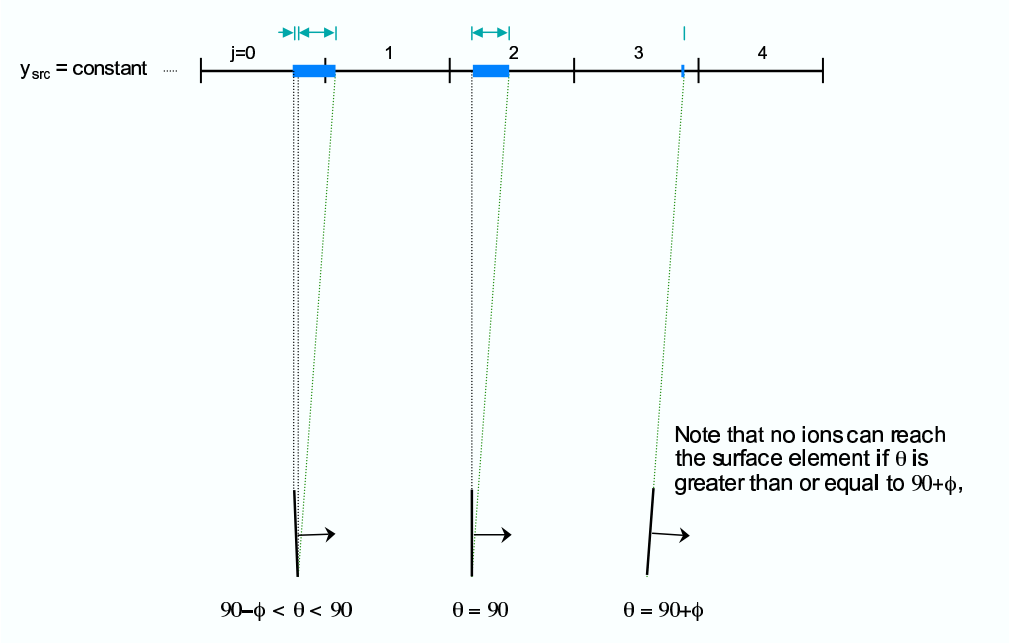

Figure 8. Illustration of how surface element orientation angles effect directional view factor geometry when $\theta > 0$

Figure 8 illustrates how certain special cases must be treated in 2D when the spreading angle is non-zero and when the orientation angle is close to 90 degrees. Note that analogous situations arise for θ near -90 degrees.

In 3D problems, accounting for the small effect of the spreading angle is more geometrically complicated. Because the spreading angle (and thus the corresponding contribution to transport) is typically quite small, the speading angle effect is neglected for 3D problems in ChISELS 1.0.

The value of G_{ij}^{d0} can be calculated as

$$G_{ij}^{d0} = B_{i,j} cos(\theta_i) \frac{Aw_{i,j}}{A_j} \tag{38}$$

where $Aw_{i,j}$ is the area of the source window that overlaps the source element j, and $B_{i,j}$ is a simple blockage function. $B_{i,j}$ is identically equal to 1 unless the direct line of sight between the surface element and the source element is blocked, in which case it is zero. In ChISELS 1.0, this is determined by looking at the values of the regular viewfactors, i.e., $B_{i,j} = 1$ if $G_{ij} > 0$, and $B_{i,j} = 0$ if $G_{ij} = 0$. Note that Equation (38) includes a $cos(\theta_i)$ term so that the flux density is properly adjusted to account for the orientation angle.

Computing $Aw_{i,j}$ requires a Boolean operation between the area of the source window and the area of each source element. For 2D ChISELS runs, this is a relatively straightforward 1D problem that consists of comparing the locations of two 1D line segments for overlap. For 3D ChISELS runs, this is a 2D problem that consists of comparing the locations of two triangular regions for overlap. To simplify this problem in 3D, ChISELS 1.0 approximates this by comparing the rectangular "bounding box" regions associated with the two triangles. Although in most cases this approximation will have very little impact, future versions of ChISELS will replace this approximation with an exact Boolean operation.

ChISELS 1.0 also assumes that the ion flux at the source plane is uniform and that it originates from a constant-y plane. Under these conditions the ion flux density received at element *i* can be computed more simply as

$$F_{ik} = F_k^{d0} cos(\theta_i) \frac{\sum_j \left(B_{i,j} Aw_{i,j} \right)}{A_{i,window}} \tag{39}$$

where F_k^{d0} is the constant emission source flux density and $A_{i,window}$ is the total area of the window in the source plane from which ions can directly reach element *i* (as illustrated in Figures 7 and 8).

3.2 Level-Set Solution Method

In ChISELS, the level-set partial differential equation, Equation (36), is solved by the so-called semi-Lagrangian method—an augmented method of characteristics for wave equations with a non-constant wave velocity [1]. This is a method of the predictor-corrector type, and thus each time step has two parts, or stages. This method was chosen because it works well for hyperbolic systems.

Galerkin's method or finite difference techniques with implicit time integration work poorly with hyperbolic systems unless upwinding or other stabilizing methods are used. An added bonus is that there is no matrix to invert. This approach requires very little memory and little inter-processor communication, thus it is amenable to parallel implementation. Also, because only interpolation is required, there are less stringent requirements of the grid.

The two stage nature of the time-stepping algorithm and each of the associated key substeps is illustrated in Figure 9. Each stage begins by computing a matrix of viewfactors, G_{ij}, between each surface i and all other surfaces j. As described above in Section 3.1 this is currently done by calling routines in Chaparral [9].

(1) Predictor stage:
  (a) Compute viewfactors for existing surfaces.
  (b) Solve for incident fluxes on each surface.
  (c) Convert fluxes to surface velocities.
  (d) Compute level set solution on grid.
  (e) Create new set of surfaces for the new level set solution.

(2) Corrector stage:
  (a) Compute new viewfactors for predicted surfaces.
  (b) Solve for incident fluxes.
  (c) Convert fluxes to surface velocities.
  (d) Compute level set solution on grid.
  (e) Create final set of surfaces for the new level set solution.

(3) Remesh around final surfaces if necessary to create new grid.

Figure 9. Breakdown of a CHISELS time step.

Parts (b) and (c) of each stage are implicitly coupled through the reaction rates at the surface. In the BTRM model, the flux, F_{ik}, of a species, k, to a surface, i, is

$$F_{ik} = F_{ik}^0 + G_{ij}\left(F_{jk} + R_{jk}\right) \tag{40}$$

where F_{ik}^0 is the direct flux from the reactor gas-phase region, G_{ij} is the view factor between surface i and j on the feature, F_{jk} is the flux of species k to surface j, R_{jk} is the production rate of species k on surface j. Repeated indices in the product of Equation (40) imply summation.

Because the surface reaction rates are a function of the species fluxes, Equation (40) is nonlinear and so must be solved iteratively. As described by Walker [11], the chosen iterative solution strategy varies by species and is a function of the magnitude of the reaction rate relative to the incident flux.

When most of the species flux is consumed by the surface reaction, i.e., $(F_{jk}+R_{jk}) \approx 0$. For this case, the initial guess of the solution is $\mathbf{F}^1 = \mathbf{F}^0$, and then iterated by

$$\mathbf{F}^{n+1} = \mathbf{F}^0 + \mathbf{G} \cdot (\mathbf{F}^n + \mathbf{R}(\mathbf{F}^n)) \tag{41}$$

where the superscript, n, denotes the iteration counter.

When only a small fraction of the species flux is consumed by the surface reaction, *i.e.*, $(F_{jk}+R_{jk}) \approx F_{jk}$ or if the production rate is very high, *i.e.* $(F_{jk}+R_{jk}) >> F_{jk}$, the initial guess is the same as before, but the iteration has the following form,

$$\mathbf{F}^{n+1} = (\mathbf{I}-\mathbf{G})^{-1} \cdot \left(\mathbf{F}^0 - \mathbf{G} \cdot \mathbf{R}\left(\mathbf{F}^l\right)\right) \tag{42}$$

In ChISELS, the linear equation system in Equation (42) is solved using standard linear algebra routines found in the AZTEC and Epetra libraries [18].

At each iterative step, the raw residual, *i.e.* the lack of closure in Equation (40), is evaluated. Iteration proceeds until that residual is smaller in magnitude than a specified threshold (currently a value of 1.e-6)).

In ChISELS, the iterative method of choice is determined by the ratio $|R|/F$ for each species individually. When $0.5 < |R|/F < 1.5$, Equation (41) is used. When $|R|/F < 0.5$ or $|R|/F > 1.5$, Equation (42) is used.

At each point in the nonlinear iteration, the reaction rates are computed as described in Section 2.3. The surface velocities are computed as the quotient of the product of production rate and molecular weight and mass density. The surface velocities are in turn used as a basis for constructing the extension velocity field needed by the level-set equations, cf. Equation (36). Once the extension velocity has been computed at the current time step, the predicted level-set function, $\tilde{\phi}$, at the next time is computed from

$$\tilde{\phi}(\mathbf{x}, t+\Delta t) = \phi(\mathbf{x} - \mathbf{v}\Delta t, t) \tag{43}$$

where Δt is the duration of the time step.

Stage 2 of a time step, the corrector stage, is nearly identical to the predictor stage. The only difference is that the calculations of transport and chemical reaction are carried out on the predicted set of surfaces. From the calculations on this surface set, an extension velocity, $\tilde{\mathbf{v}}$, is computed. The corrected level-set function at the next time step is then computed via

$$\phi(\mathbf{x}, t+\Delta t) = \phi\left(\mathbf{x} - \frac{1}{2}(\mathbf{v}+\tilde{\mathbf{v}})\Delta t, t\right). \tag{44}$$

A time step is completed by determining if the surface has moved enough to warrant remeshing in order to maintain the level of spatial resolution specified by the user. If remeshing is required, a new quad-tree (2D) or oct-tree (3D) mesh is generated as described in the initialization stage, and the domain is decomposed and redistributed among processors to maintain a balanced computa-

tional load.

3.3 Dynamic Mesh Refinement

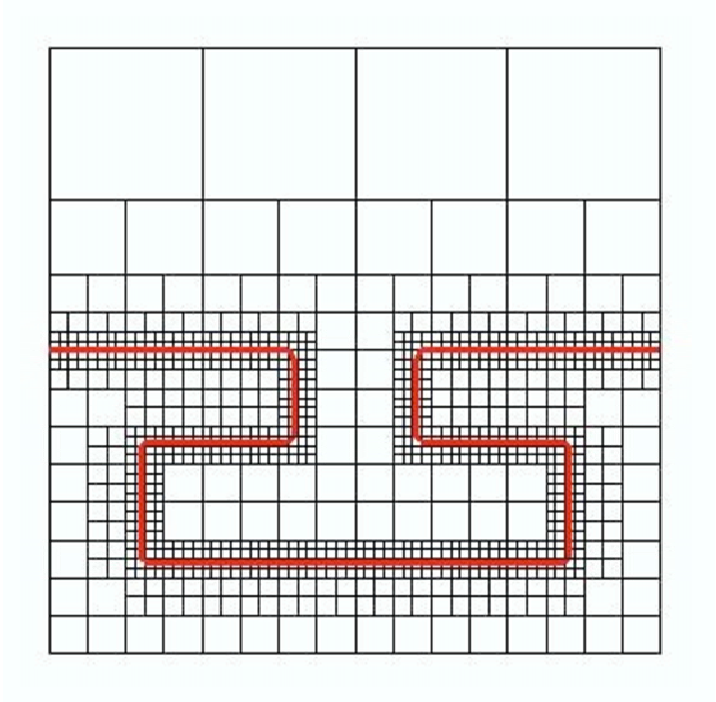

Figure 10. Illustration of 2D grid refinement near a surface.

The meshes used in ChISELS are quad-trees (2D) and oct-trees (3D). These types of meshes are convenient when mesh refinement is only needed in certain areas, such as near an interface. The genesis cell bounds the entire computational domain; the code recursively subdivides the cells according to the criterion

$$d/l < \varepsilon \tag{45}$$

where l is the length of the cell side and d is the distance from the center of the cell to the nearest surface. In this fashion, quad-tree (2D) or oct-tree (3D) meshes are quickly generated that concentrate mesh points around the surface where accurate solution of the level-set equation is most required. The refinement proceeds until a user-specified length tolerance is obtained or a maximum level of recursion is completed.

An example mesh illustrating this type of grid refinement is shown in Figure 10.

For 2D problems, the surface elements are defined by the mesh-line intersection points implied by the level-set function values. Linear interpolation is used in finding these intersection points. For 3D problems a marching cubes algorithm [19] is employed to compute elements of the level set or surface on the refined grid.

3.4 Parallelization and Load Balancing Strategy

Because ChISELS is intended to handle the largest possible class of problems, all implementations of the theoretical models and solution algorithms are designed to scale efficiently to hundreds of processors. Specifically, ChISELS is written for use on distributed memory Multiple Instruction Multiple Data (MIMD) computer systems that have a standard MPI library [20] installed. However, running ChISELS in parallel is optional, and ChISELS can also be built and used on single-processor computers.

An important aspect of parallel programming is the approach taken to distribute the work load among the available processors. The trick is to balance the amount of work assigned to each processor so that all processors remain busy all of the time. In ChISELS, a domain decomposition strategy is employed. In this context, domain means the computational domain, and implies that each processor is assigned to do any work and store any memory associated with a specific region of the mesh. If the work load and memory requirements are uniformly distributed and static in time, then the domain decomposition problem is trivial. However, when the work load varies in time and evolves spatially during the computation, such as occurs in a ChISELS problem as the evolving surface moves, then special care must be taken to monitor the work load and adjust the domain decomposition accordingly.

In practice the code begins a calculation by sub-dividing the computational domain equally amongst all available processors. However, after each mesh refinement step, the work load is evaluated. Because only in rare circumstances will the cells be evenly divided among processors after the mesh refinement is completed, a Sandia-developed parallel load-balancing library, Zoltan [21][22], is called upon to redistribute the cells across processors. Figure 11 shows a quad-tree refinement about a surface and the domain decomposition after load balancing.

As mentioned above, a marching cubes algorithm [19] is employed to compute elements of the level set or surface on a refined 3D grid. Once again, not all processors own an equal number of surface elements and some of the computational work scales with the number of surfaces, so Zoltan routines are also called upon to redistribute the surfaces across processors.

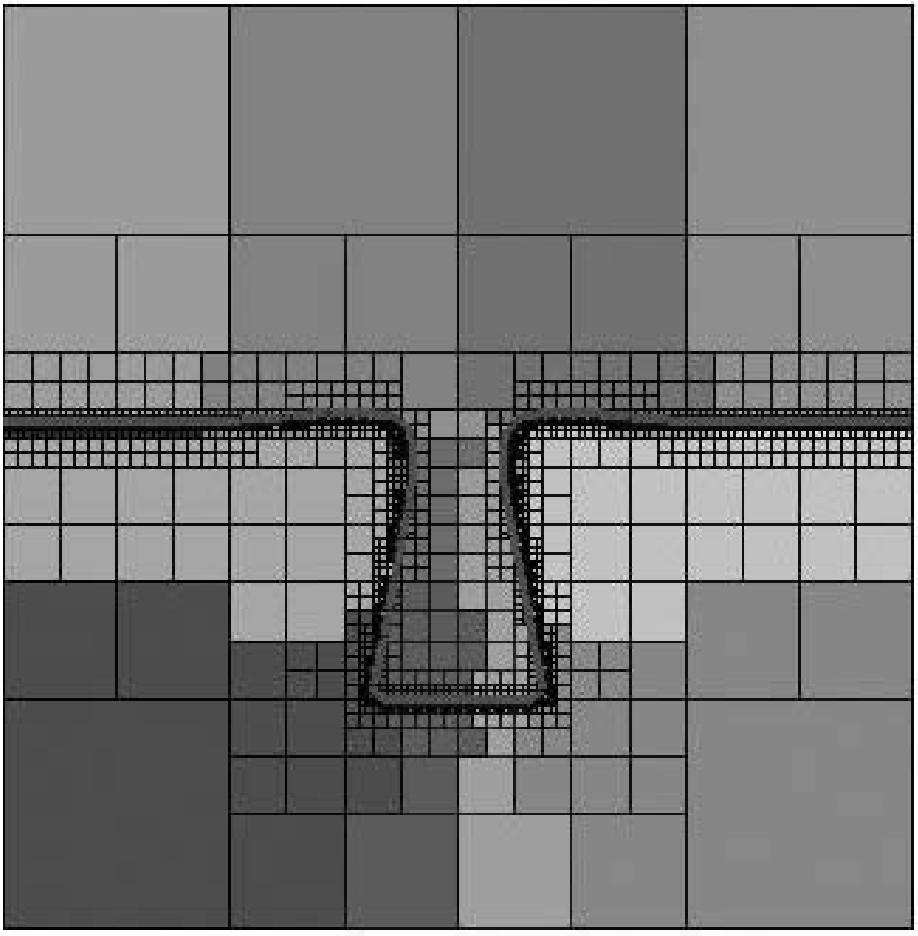

Figure 11. Snapshot of a 2D ChISELS 1.0 simulation showing the surface, the refined quad-tree grid around the surface, and the assignment of grid cells to processors after load-balancing. Each of 16 processors owns a different gray-shaded region of the grid.

4 Users Guide

4.1 Obtaining, Building, and Running ChISELS 1.0

ChISELS 1.0 is copyrighted by Sandia National Laboratories and licensed under a GNU lesser general public license (as published by the Free Software Foundation). This is a particular type of open-source licensing agreement with specific requirements that can be reviewed at the following GNU web site, www.gnu.org/licenses/lgpl.html. At present, ChISELS 1.0 can be obtained by contacting either of the first two authors of this report at Sandia National Labs. Authorized recipients will be sent or given access to a compressed tar file containing the directories and files needed to install and build ChISELS 1.0 on one of the supported platforms. Platforms currently supported include Linux, SGI (Irix 6.5), Mac (OS 10.3), and the Institutional Computing Clusters (ICC). Instructions for installing the code in different configurations will be included. All input files required for the example problems described in Section 4.4 are also available.

ChISELS 1.0 is designed to link with SURFACE CHEMKIN, which must be obtained and installed separately because it is a commercially licensed software. However, this is not required and if the user desires, they can modify the appropriate routines to solve problems without the use of SURFACE CHEMKIN. Also, ChISELS may be run on either parallel or serial workstations. However, to use multiple processors in parallel, an MPI library must be available on the local machine and the code must be linked to the MPI libraries when it is built.

ChISELS 1.0 is designed to be run in command line mode from a simple terminal window on a UNIX based computer. Once installed and built on a local machine, it is run by typing the command

chisels *infile*

where **chisels** is the name of the executable version of ChISELS 1.0, and ***infile*** is the name of the main input file. The main input file contains problem specific settings that enable the user to define the problem being solved, control various modeling parameters, and control the output generated during and after a simulation. Various other input files are also required as explained in the next section.

4.2 Input Files

At a minimum, ChISELS 1.0 requires two valid input files in order to run; (1) a main command-line input file, and (2) a problem geometry input file. As explained above, when invoking ChISELS 1.0 in UNIX , the name of the main input file must immediately follow the **chisels** command. The name of the problem geometry input file is specified from within the main input file. In addition, if the CHEMKIN package is being used to define chemical mechanisms, a CHEMKIN input file and a SURFACE CHEMKIN input file must be present and properly specified from within the main input file.

4.2.1 Main Input File

The main input file uses a simple text-based command line format with the following syntax:

One command per line.
Lines starting with # are comments and blank lines are allowed.
Command names must be lower case
Commands can be in any order.
The command name must start in 1st column
The rest of command is free-form and can use spaces or tabs to separate arguments
If not changing the default, a command need not be listed

Available commands can be categorized into four different groups: (1) Problem definition, (2) Time step and run-time controls, (3) Output controls, and (4) Modeling controls and specifications. The following is a list of each valid command in the four groups, and includes a brief description of the command, the number of arguments required, and the default value(s) of the argument(s) if the command line is not specified.

Problem Definition Commands

COMMAND	DESCRIPTION	# ARGS.	DEFAULT
dimension	Dimensionality (2 or 3) of the problem	1	2
initial surfaces	Name of the problem geometry input file which defines the initial surface locations	1	in.geom
chemkin input	Name of the CHEMKIN file required if linking to CHEMKIN	1	*no default*
surface chemkin input	Name of the SURFACE CHEMKIN file required if linking to CHEMKIN	1	*no default*
number gas species	The number of gas-phase species	1	1
mole fraction	Name of gas-phase species and its mole fraction	2	*no default*, 0.0
ion energy	Name of positive ion species followed by an ion energy (eV)	2	*no default*, 0.0
temperature	Gas-phase, ion, and electron temperatures (K)	3	*no defaults*
gas pressure	Thermodynamic pressure of the gas-phase (torr)	1	*no default*
bohm	A correction factor ξ for the Bohm condition (see Eq. 31 relating to ion surface reactions)	1	1.0
spreading angle	The spreading angle defined in Figure 7 for the directional transport of positive ions (degrees)	1	2

Notes to Problem Definition Commands:

The names used in the “mole fraction” and “ion energy” command lines must be valid species. Species not listed in the input file using these commands are given the default value of zero.

The effect of spreading angle on directional transport of ions is not accounted for in 3D calculations.

Time Step and Run-time Controls

COMMAND	DESCRIPTION	# ARGS.	DEFAULT
timestep	Size of timestep (seconds)	1	0.001
ending time	Execution stops if time exceeds this value (seconds)	1	1.e99
adjust dt flag	Time step auto-adjustment flag. If set to 0, the time step is constant, otherwise it will be automatically adjusted based on grid size and surface velocities	1	1
adjust dt multiplier	Maximum fractional change in time step allowed each time step if adjust dt flag is non-zero.	1	0.2
number of steps	Total number of timesteps to take before stopping	1	40

Output Controls

COMMAND	DESCRIPTION	# ARGS.	DEFAULT
vtk_out	If non-zero, a vtk graphics output file is created	1	0
vtk_filename	Name of vtk output file	1	vtkout
vtkcompressed_out	If non-zero, vtk output is compressed	1	0
qt_out	If non-zero, a qt graphics output file is created	1	0
qt_filename	Name of qt output file with surface/cell info	1	out.geom
qt cell output	If > 0, a background mesh description is placed in the qt output file for visualization purposes. The value specifies the number of steps between inclusions.	1	0
screen	Screen output flag. It directs local output to the screen, with a verbosity level based on its value: = 0, > 3, or $<$ -5 no output = 1, 2 or 3 increasing amount of performance info. = -1 to -5 increasing amount of debugging info.	1	1
logfile	Logfile output flag. It directs local output to a file named ***infile.log***, with a verbosity level based on its value (see screen command for details).	1	0

Notes to Output Controls:

The vtk output file is written in a form suitable for ParaView, an open-source, multi-platform visualization application (see www.paraview.org).

The qt output file is written in a form suitable for a simple Qt-based [23] visualization tool written by and used by the ChISELS developers (not distributed with Chisels 1.0)

The “screen” and “logfile” commands are mutually exclusive. If both appear in the input file, the one that comes last will control the output. Also, verbosity levels of -4 and -5 produce an extremely large amount of output, and should be used with care and only when large amounts of output can be handled.

Modeling Controls and Specifications

COMMAND	DESCRIPTION	# ARGS.	DEFAULT
global box	Bounding box coordinates (μm) of the domain for 2D: xlo, ylo, xhi, yhi for 3D: xlo, ylo, zlo, xhi, yhi, zhi	4 or 6	-5. -5. 5. 5.
source side	Specifies which side of the computational domain corresponds to the gas-phase source of chemical species 0: side located at z= zlo, 3: side located at y= yhi 1: side located at y= ylo, 4: side located at x=xlo 2: side located at x=xhi, 5: side located at z= zhi	1	3
source elements	Number of uniform elements used to discretize the gas-phase source side of the computational domain. If not specified in a command line, this is found as: $2^{(N_{gl})}$, where N_{gl} is given in the "grid levels" command.	1	*see text*
grid levels	Max number of levels to recurse in the quadtree for local mesh refinement as the surface evolves.	1	5
remesh interval	Number of steps between remeshing. Used to maintain local mesh refinement as the surface evolves.	1	3
redistance interval	Number of steps between redistancing operations	1	3
vf drop tolerance	View factor drop tolerance	1	1.e-4
yield_cosine	Optional cosine-based yield factor function for ion enhanced surface reactions. See Equation (33).	0	na
yield_poly	Optional polynomial-based yield factor function for ion enhanced surface reactions. See Equation (34). Arguments specified are the peak value and corresponding angle (radians) as illustrated in Figure 6b.	2	na
yield_trig	Optional trigonometric-based yield factor function for ion enhanced surface reactions. The five arguments specified are the constants A, B, C, D, and E in Equation (35).	5	na
yield_spline	Optional spline-based yield factor function for ion enhanced surface reactions. The three arguments specified are (a) the length of the uniform flat region, (b) the location of the peak, (c) the magnitude of the peak (see Fig. 6d).	3	na

Notes to Modeling Controls and Specifications:

For problems with preferred direction transport of ions, the source side must be 3.

If an argument to "source elements" of less than two is specified, the code uses the default formula based on grid levels.

Redistancing is the process of generating a discrete level-set field corresponding to a signed distance function.

The view factor drop tolerance is only used if convergence problems are detected in the ballistic transport model. If convergence fails, the code will attempt to re-solve the problem after dropping

all view-factors in the view-factor matrix that are less than this tolerance value.

The yield factor function commands are mutually exclusive. If more than one is specified in the input file, the one that comes last will control what the code does. If none are specified, then the yield factor function is set equal to 1.0.

4.2.2 Geometry Input File

The geometry input file defines the initial state of the surface, and it must be present in order to run ChISELS. By default it is called "in.geom," but it can be given any other name by using the "initial surfaces" command in the main input file.

Each line in the file must be either a blank line (which is ignored), a comment line, which starts with #, or a one-line description of a surface element. For 2D problems the surface element description consists of two integer values followed by six real numbers. The first integer is used to identify the element, and thus must be unique to the element. The second integer must be present but is currently not used for any purpose in the code (e.g. it can always be set to 0). The next four numbers define a pair of x,y endpoints of the element where the units are assumed to be microns (i.e. 1.e-6 meters). The last two real numbers define the x and y components of the surface normal vector. The format is free-form, meaning that either spaces or tabs can be used to separate arguments. Also, elements can be specified in any order, but must, as a group, define a contiguous surface spanning the boundaries of the computational domain and be properly oriented relative to the source side defined in the main input file.

The following is an example 2D input geometry file that defines a flat surface with a small notch within the boundaries of the default computational domain and the default source side.

```
# ITEM: SURFACES
# (Values in microns)
#    X1  Y1   X2  Y2   Ni  Nj
1 0 -5.0 2.0 -1.0 2.0  0.0 1.0
2 0 -1.0 2.0 -1.0 0.0  1.0 0.0
3 0 -1.0 0.0  1.0 0.0  0.0 1.0
4 0  1.0 0.0  1.0 2.0 -1.0 0.0
5 0  1.0 2.0  5.0 2.0  0.0 1.0
```

Lines defining elements for 3D problems consist of two integer values followed by twelve real numbers. The first integer is used to identify the element, and thus must be unique to the element. The second integer must be present but is currently not used for any purpose in the code (e.g. it can always be set to 0). The next nine real numbers define three x,y,z coordinate sets that define the endpoints of a triangular element (in microns). The last three real numbers define the x, y and z components of the surface normal vector.

Creating input geometry files, particularly for complicated surface geometries or for 3D prob-

lems, can be tedious and difficult. Furthermore, ChISELS 1.0 does not have routines to check the input file for consistency, such as with the boundaries of the computational domain or that normals are specified correctly, or whether the elements form a complete contiguous surface without holes. Therefore, a user must take special care to assure that this file is accurate and complete, or unpredictable and erroneous results and/or error messages may be produced by the code.

4.2.3 CHEMKIN Input Files

As described above in Sections 2.3 and 2.4, heterogeneous chemical reactions at the interface between a solid surface and an adjacent gas are the physical basis for the deposition and etching processes modeled by ChISELS. To facilitate the modeling of these reactions, ChISELS is designed to couple to the CHEMKIN software [2]. This requires a set of two CHEMKIN compatible input files that define the gas phase chemistry and the surface chemistry reaction mechanisms that are being treated. The names of these two files are specified in the main input file by use of the "chemkin input" and "surface chemkin input" commands.

The CHEMKIN input files define all of the chemistry occurring in the system. The gas-phase input file provides the chemical composition of the various gas-phase species in the mechanism as well as their thermochemical properties, the chemical reactions the species participate in, and the rates of those reactions. The surface chemistry input file does the same for surface/bulk species and reactions. The mechanics of including chemical information in the input files, including a description of data formats, is covered in the CHEMKIN Input Manual, while the CHEMKIN Theory Manual describes the formulation of the various forms of the chemical rate expressions (see reference [2]).

The user is required to provide the chemical data in the reaction mechanism. If the system of interest has been modeled by previous workers in the field, it may be possible to find a complete set of files that describe the system of interest, or published literature that provides a reaction mechanism. A number of the deposition and etching processes used in the SUMMIT-V technology have previously been studied. Further information can be obtained by contacting the third author of this report.

4.3 Output Files and Visualization Tools

There are two different kinds of output generated by ChISELS 1.0. The first type contains information concerning how the run is progressing. It can be directed either to the screen (by use of the "screen" command) or to a logfile (by use of the "logfile" command). The amount of information that is produced is controlled by the associated argument in the input file, as described above in Section 4.2.

Data visualization files are the second type of output generated by ChISELS. Visualization of the evolving surface, either as static "snapshots" at various points in time, or as a temporally evolving animation, is the primary mechanism for evaluating the results of a ChISELS run. If the

"vtk_out" command is specified in the input file, then a vtk output file is written in a form suitable for ParaView. ParaView is a powerful open-source, multi-platform visualization application available for download off the web at www.paraview.org. The name of the output file is specified by using the "vtk_filename" command, and the file (which can be quite large) will be automatically compressed if the "vtkcompressed_out" command is used.

When the "qt_out" command is invoked, an output file is written in a form suitable for a simple Qt-based visualization tool written and used by the ChISELS developers during code development. Qt is an open source C++ application development framework available online at http://www.trolltech.com/products. Because the file created is a text file and produces a list of surface elements in exactly the same form needed for the input file, this output can also be used to manually create a geometry input file that can effectively serve as a restart file. An automated restart capability is planned for later versions of ChISELS.

4.4 Example Problems

4.4.1 Silane Deposition in a Simple 2-D Trench

This example is a simulation for the LPCVD of undoped silicon from a silane precursor. This process is quite important in SMM as it is used to deposit the main structural material, polysilicon. This CVD process produces very conformal films, which we demonstrate using a simple 2D trench.

Figure 12 gives listings of the ChISELS input command file and "in.geom_notch", the geometry input file. This example is for a temperature of 853 K = 580 C and a total pressure of 0.4 Torr, which are realistic LPCVD conditions. In this problem ChISELS is linked to CHEMKIN, so the input command file includes CHEMKIN and Surface-CHEMKIN input file names. Figure 13 gives a listing of smallche.inp, the gas-phase chemistry input file, while Figure 14 gives a listing of smallsur.inp, the surface chemistry input file.

The reaction mechanism used in this example contains only three gas-phase chemical species, one gas-phase reaction, two surface species, one bulk species, and three surface reactions. This mechanism is a very simplified version of a full mechanism developed at Sandia for silane CVD; see references [24], [25], [26], [27] and [28] for details of the mechanism development process. The gas-phase species are SiH_4, the silane input gas, SiH_2, a reactive intermediate (silylene) that is formed by decomposition of silane, and H_2, a byproduct formed by decomposition of silane (in the gas or on the surface). The gas-phase reaction, the collisionally-induced decomposition of silane, is included in the mechanism file, but is not actually considered in this simulation. As indicated by the mole fraction input commands in Figure 12, the input gas to the feature-scale simulation consists of silane only. The two surface species, SI(S) and SIH(S), represent open sites on the silicon surface, and hydrogen-covered surface sites, respectively. The bulk species, SI(D), represents solid silicon that has been chemically deposited. The silane deposits silicon on the surface in a two step process. First the silane reacts with open sites on the surface to form hydrogenated surface sites, one bulk silicon, and one gas-phase hydrogen product. Then the hydrogenated surface sites react with each other to eliminate another hydrogen molecule and regenerate the open silicon surface sites. The

reaction of SiH_2 on the surface is also included in the mechanism. This species reacts at the surface with much higher efficiency than silane and would lead to very non-uniform deposition if a significant quantity of this species is included in the input gas mixture.

Figure 15 shows: a) the starting (t=0) trench surface and level-set grid, b) the final surface and level-set grid after a 60 minute simulation, and c) a series of surfaces at 10 minute intervals, where the time is deposition time, not simulation-run time. As expected, the deposition is very conformal (uniform), filling the trench with no holes. Note that the trench does not completely disappear; the remaining dimple is consistent with experiment. It results from the fact that uniformly depositing over a corner does not propagate the corner in all directions, but rather results in a rounded, curved surface.

```
# Input Command file for Silane deposition in
# a simple 2-D trench
#
# Problem Definition Commands
# -------------------------------------------
dimension               2
initial surfaces        in.geom_notch
chemkin input           smallche.inp
surface chemkin input   smallsur.inp
number gas species      3
mole fraction           SIH4   1.0
mole fraction           SIH2   0.0
mole fraction           H2     0.0

temperature             853.0  0.0  0.0
gas pressure            0.4

# Time Step and Run-time controls
# -------------------------------------------
timestep                60.0
adjust dt flag          0
number of steps         61

# Output Controls
# -------------------------------------------
qt output               1
cell output             10
qt_filename             out.geom_notch
screen                  1

# Modeling Controls and Specifications
# -------------------------------------------
global box              -1.0 -1.0 1.0 1.0
source side             3
grid levels             6
```

(a) Input command file

```
# Initial Surface definition for Silane
# deposition in a simple 2-D trench
# (Values in microns)
#    X1   Y1   X2   Y2   Ni  Nj
1 0 -1.0  0.0 -0.2  0.0  0.0 1.0
2 0 -0.2  0.0 -0.2 -0.6  1.0 0.0
3 0 -0.2 -0.6  0.2 -0.6  0.0 1.0
4 0  0.2 -0.6  0.2  0.0 -1.0 0.0
5 0  0.2  0.0  1.0  0.0  0.0 1.0
```

(b) Geometry Input file

Figure 12. Listing of the main input file and the geometry input file for example problem 1.

```
ELEMENTS
SI H
END
SPECIES
SIH4 SIH2
H2
END
THERMO ALL
  300.     1000.     2000.
SIH2               80387H   2SI  1    0    0G   300.000  2000.000 1000.00      1
 0.37376173E+01 0.26652140E-02-0.10297152E-06-0.53034788E-09 0.14005514E-12    2
 0.31021018E+05 0.25981410E+01 0.33826566E+01 0.25535191E-02 0.38814477E-06    3
 0.24234970E-09-0.65710301E-12 0.31234377E+05 0.48579831E+01                   4
SIH4               90784SI  1H   4    0    0G   300.000  2000.000              1
  .79359380E+00  .17671899E-01 -.11398009E-04  .35992604E-08 -.45241571E-12    2
  .31982127E+04  .15242257E+02  .14516404E+01  .13987363E-01 -.42345639E-05    3
 -.23606142E-08  .13712089E-11  .31134105E+04  .12321855E+02                   4
H2                 J 3/77H   2    0    0    0G   300.000  5000.000              1
   .30558123+01   .59740400-03  -.16747471-08  -.21247544-10   .25195487-14    2
  -.86168476+03  -.17207073+01   .29432327+01   .34815509-02  -.77713819-05    3
   .74997496-08  -.25203379-11  -.97695413+03  -.18186137+01                   4
END

REACTIONS
SIH4(+M)=SIH2+H2(+M)           0.3119E+10   1.669  54710.    ! R1
   LOW  / 0.5214E30  -3.545  57550./
   TROE / -0.4984  888.3   209.4   2760./
   SIH4/4./
! HF(SiH2)=64.3, anh_inc.16b,  beta(Ar,300) = 0.25 fit from 300 to 1200K
!
END
```

Figure 13. Listing of the CHEMKIN input file for example problem 1.

```
!Dissociative Adsorption, Hydrogen desorption mechanism
!to be used with evengas mechanism
!fit to our rsc data 27 Jun 91
!hydrogen desorption from PRL 62(89)567
!version 2: uses COV trick to get first order reaction
!1.754E20 = 7.9e11/(2 * SDEN)
SITE/SILICON/          SDEN/2.2524E-09/
  SI(S)
  SIH(S)
END
BULK   SI(D)         /2.33/
END
THERMO ALL
  300.      600.     1685.
SI(S)             J 3/67SI  1    0    0    0S   300.000  1685.000             1
 0.24753989E 01 0.88112187E-03-0.20939481E-06 0.42757187E-11 0.16006564E-13    2
-0.81255620E 03-0.12188747E 02 0.84197538E 00 0.83710416E-02-0.13077030E-04    3
 0.97593603E-08-0.27279380E-11-0.52486288E 03-0.45272678E 01                   4
SIH(S)            J 3/67H   1SI  1    0    0    0S   300.000  1685.000             1
 0.24753989E 01 0.88112187E-03-0.20939481E-06 0.42757187E-11 0.16006564E-13    2
-0.81255620E 03-0.12188747E 02 0.84197538E 00 0.83710416E-02-0.13077030E-04    3
 0.97593603E-08-0.27279380E-11-0.52486288E 03-0.45272678E 01                   4
SI(D)             J 3/67SI  1    0    0    0S   300.000  1685.000             1
 0.24753989E 01 0.88112187E-03-0.20939481E-06 0.42757187E-11 0.16006564E-13    2
-0.81255620E 03-0.12188747E 02 0.84197538E 00 0.83710416E-02-0.13077030E-04    3
 0.97593603E-08-0.27279380E-11-0.52486288E 03-0.45272678E 01                   4
END

REACTIONS
   SIH4     + 2SI(S) => 2SIH(S) +  SI(D) + H2   8.39E26    0.0   37450.0
   2SIH(S)           => 2SI(S)  +  H2           1.754E20   0.0   47000.0
                                                COV/SIH(S) 0.0 -1.0 0.0/
   SIH2              => SI(D)   +  H2           1.0        0.0   0.0
                                                STICK
END
```

Figure 14. Listing of the Surface CHEMKIN input file for example problem 1.

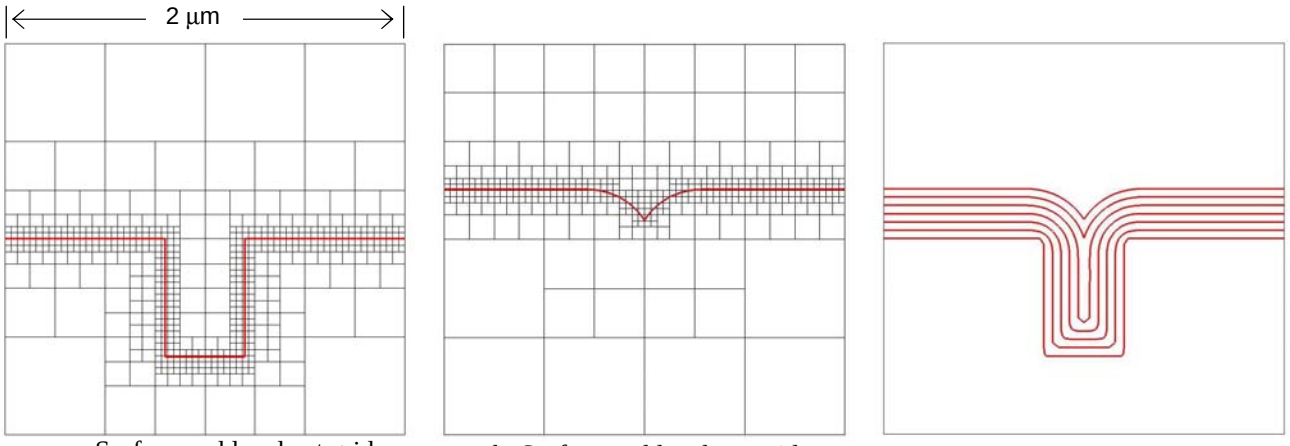

a. Surface and level-set grid at t = 0 min.

b. Surface and level-set grid at t = 60 min.

c. Surface at t = 0, 10, 20, 30, 40, 50, and 60 min.

Figure 15. Sample output from Silane deposition in a simple 2-D trench.

4.4.2 PECVD of SiO_2 from Ar, O_2 and SiH_4 in a High Aspect Ratio 2-D Trench

This example is a simulation for the deposition of silicon dioxide from a silane, oxygen and argon plasma. This process is used to deposit oxides at lower wafer temperatures than would be needed for a thermal oxide deposition process, but results in substantially non-uniform deposits. We use a simple 2D trench in the example, but one with a higher aspect ratio (10:1). This PECVD process involves the deposition of oxide by radicals created in the plasma, occurring simultaneously with ion-assisted deposition and sputtering/etching of that deposit by ions from the plasma. The goal is to fill trenches, or other features, with oxide, while minimizing the size of the holes left behind if the deposition is too non-conformal.

Figure 16 gives listings of the ChISELS Input command file and "in.geom_notch10X1", the geometry input file. This example involves a non-equilibrium plasma, so three temperatures are provided: The neutral species are at room temperature (300 K), the ions have a higher temperature of 5000 K, and the electrons have a much higher temperature of 28651 K or 2.47 eV. Note that the ion energies are input separately, and reflect the bias voltage applied to the substrate, rather than the ion temperature.

This example problem is for a case where ChISELS is linked to CHEMKIN, so the input command file includes CHEMKIN and Surface-CHEMKIN input file names. Figure 17 gives a partial listing of chem_sio2.inp, the gas-phase chemistry input file, while Figure 18 gives a partial listing of surf_1matl.inp. the surface chemistry input file. This example involves a fairly complex chemical reaction mechanism with 46 gas-phase species, 168 gas-phase reactions, 13 surface species, one bulk species, and 194 surface reactions. This mechanism is described in detail in [29], but we note that it was developed using reactor-scale data only. In this case, the mole fractions being input into ChISELS are results from a 0D reactor-scale simulation of the PECVD process [2].

Figure 19 shows: a) the starting (t=0) trench surface and the refined level-set grid, and b) the initial deposition rates as a function of position in the trench for three different ion energies. In the latter, all points along the bottom of the trench are plotted at x = -10, so there are multiple points there for each ion energy. The non-uniform deposition observed in this figure is the result of several physical phenomena. The ion energy of 15 eV is below the sputtering threshold, so the deposition rate at the bottom of the trench is higher than that on the sidewall as a result of ion-assisted deposition reactions. In the 15 eV case, the additional deposition at the top of the trench results from reactive radical species that have been formed in the gas (that get depleted near the top of the trench), plus a contribution from ion-assisted surface reactions (the ions have a few degrees of spread, so some hit the sides of the trench). An ion energy of 40 eV is just above the threshold for ion-sputtering reactions, and ion sputtering competes with ion-assisted deposition on the bottom of the trench, lowering the net deposition rate there. The sputtered material re-deposits on the sidewalls. In the case of the 60eV ion energy, the ions predominantly sputter material off the bottom of the trench for net etching, adding even more re-deposited material to the sidewalls. Note that these simulations were done with no angular dependence to the yield of ion-assisted reactions, which is physically somewhat unrealistic. Use of a different yield factor functions would give different results.

```
# Input command file for PECVD of SiO2 from
# Ar, O2, and SiH4
# 10x1 aspect ratio trench,
# P = 0.03 Torr,  Ion Energy = 15 eV

# Problem Definition Commands
# -------------------------------------------
dimension               2
initial surfaces        in.geom_notch10X1
chemkin input           chem_sio2.inp
surface chemkin input   surf_1matl.inp
temperature             300.0  5800  28651
gas pressure            0.03
number gas species      46

# Mole fractions of gas phase species
mole fraction E         0.000103034
mole fraction AR+       0.000102512
mole fraction O+        3.63E-07
mole fraction O2+       4.42E-07
mole fraction SIH3+     7.24E-08
mole fraction SIH2+     1.28E-07
mole fraction SIH+      3.28E-08
mole fraction SI+       1.50E-09
mole fraction H+        5.49E-08
mole fraction H2+       1.89E-07
mole fraction O-        7.60E-07
mole fraction SI        9.65E-09
mole fraction SI2       1.43E-09
mole fraction SIH       1.08E-06
mole fraction SIH2      3.33E-05
mole fraction SIH3      7.97E-06
mole fraction SIH4      0.000573576
mole fraction SI2H2     1.10E-06
mole fraction SI2H3     7.90E-11
mole fraction H2SISIH2  7.91E-19
mole fraction SI2H5     5.06E-06
mole fraction SI2H6     1.12E-05
mole fraction SIO       4.31E-07
mole fraction SIO2      9.15E-20
mole fraction SIH2O     6.12E-06
mole fraction HSIO      2.24E-07
mole fraction SIH3O     2.71E-16
mole fraction HSIOOH    4.90E-06
mole fraction H         0.01169274
mole fraction H2        0.01201013
mole fraction OH        2.20E-05
mole fraction H2O       5.18E-05
mole fraction HO2       0.0
mole fraction H2O2      1.93E-11
mole fraction O*        6.35E-05
mole fraction O         0.007619644
mole fraction O2        0.009235906
mole fraction O3        7.67E-10
mole fraction AR*       0.001443052
mole fraction AR        0.9570088
```

(a) Input command file

```
# Ion energies of positive ion species in
units of eV
ion energy AR+          15
ion energy O+           15
ion energy O2+          15
ion energy SIH3+        15
ion energy SIH2+        15
ion energy SIH+         15
ion energy SI+          15
ion energy H+           15
ion energy H2+          15

# Time Step and Run-time controls
# -------------------------------------------
timestep                1.0e-3
number of steps         1

# Output Controls
# -------------------------------------------
qt output               1
cell output             1
qt_filename             out.pecvd10X1P0.03
screen                  1

# Modeling Controls and Specifications
# -------------------------------------------
global box              -6.0 -11.0 6.0 1.0
source side             3
grid levels             7
```

(b) Continuation of input command file

```
# Initial Surface definition for PECVD of
# SiH2 from Ar, O2, and SiH4
# 10 X 1 aspect ratio 2-D trench
# (Values in microns)
#    X1   Y1   X2   Y2   Ni  Nj
1 0 -6.0  0.0 -0.5  0.0  0.0 1.0
2 0 -0.5  0.0 -0.5 -10.  1.0 0.0
3 0 -0.5 -10.  0.5 -10.  0.0 1.0
4 0  0.5 -10.  0.5  0.0 -1.0 0.0
5 0  0.5  0.0  6.0  0.0  0.0 1.0
```

(c) Geometry Input file

Figure 16. Listing of the main input file and the geometry input file for example problem 2.

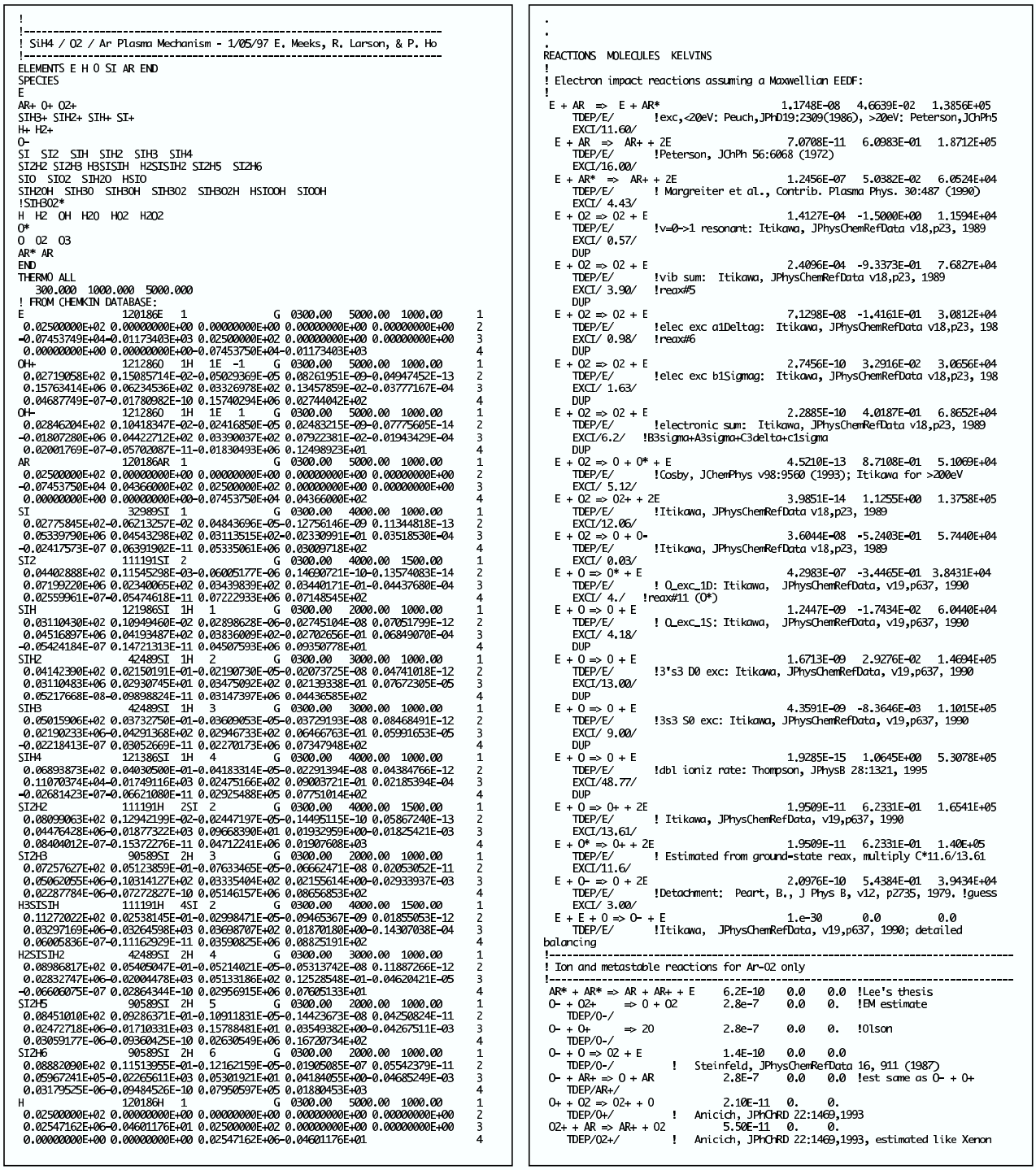

```
!
!-----------------------------------------------------------------------
! SiH4 / O2 / Ar Plasma Mechanism - 1/05/97 E. Meeks, R. Larson, & P. Ho
!-----------------------------------------------------------------------
ELEMENTS E H O SI AR END
SPECIES
E
AR+ O+ O2+
SIH3+ SIH2+ SIH+ SI+
H+ H2+
O-
SI  SI2  SIH  SIH2  SIH3  SIH4
SI2H2 SI2H3 H3SISIH  H2SISIH2 SI2H5  SI2H6
SIO  SIO2  SIH2O  HSIO
SIH2OH  SIH3O  SIH3OH  SIH3O2  SIH3O2H  HSIOOH  SIOOH
!SIH3O2*
H  H2  OH  H2O  HO2  H2O2
O*
O  O2  O3
AR* AR
END
THERMO ALL
   300.000  1000.000  5000.000
! FROM CHEMKIN DATABASE:
E                 120186E   1               G  0300.00   5000.00  1000.00      1
 0.02500000E+02 0.00000000E+00 0.00000000E+00 0.00000000E+00 0.00000000E+00    2
-0.07453749E+04-0.01173403E+03 0.02500000E+02 0.00000000E+00 0.00000000E+00    3
 0.00000000E+00 0.00000000E+00-0.07453750E+04-0.01173403E+03                   4
OH+               1212860   1H   1E  -1     G  0300.00   5000.00  1000.00      1
 0.02719058E+02 0.15085714E-02-0.05029369E-05 0.08261951E-09-0.04947452E-13    2
 0.15763414E+06 0.06234536E+02 0.03326978E+02 0.13457859E-02-0.03777167E-04    3
 0.04687749E-07-0.01780982E-10 0.15740294E+06 0.02744042E+02                   4
OH-               1212860   1H   1E   1     G  0300.00   5000.00  1000.00      1
 0.02846204E+02 0.10418347E-02-0.02416850E-05 0.02483215E-09-0.07775605E-14    2
-0.01807280E+06 0.04422712E+02 0.03390037E+02 0.07922381E-02-0.01943429E-04    3
 0.02001769E-07-0.05702087E-11-0.01830493E+06 0.12498923E+01                   4
AR                120186AR  1               G  0300.00   5000.00  1000.00      1
 0.02500000E+02 0.00000000E+00 0.00000000E+00 0.00000000E+00 0.00000000E+00    2
-0.07453750E+04 0.04366000E+02 0.02500000E+02 0.00000000E+00 0.00000000E+00    3
 0.00000000E+00 0.00000000E+00-0.07453750E+04 0.04366000E+02                   4
SI                 32989SI  1               G  0300.00   4000.00  1000.00      1
 0.02775845E+02-0.06213257E-02 0.04843696E-05-0.12756146E-09 0.11344818E-13    2
 0.05339790E+06 0.04543298E+02 0.03113515E+02-0.02330991E-01 0.03518530E-04    3
-0.02417573E-07 0.06391902E-11 0.05335061E+06 0.03009718E+02                   4
SI2               111191SI  2               G  0300.00   4000.00  1500.00      1
 0.04402888E+02 0.11545298E-03-0.06005177E-06 0.14690721E-10-0.13574083E-14    2
 0.07199220E+06 0.02340065E+02 0.03439839E+02 0.03440171E-01-0.04437680E-04    3
 0.02559961E-07-0.05474618E-11 0.07222933E+06 0.07148545E+02                   4
SIH               121986SI  1H  1           G  0300.00   2000.00  1000.00      1
 0.03110430E+02 0.10949460E-02 0.02898628E-06-0.02745104E-08 0.07051799E-12    2
 0.04516897E+06 0.04193487E+02 0.03836009E+02-0.02702656E-01 0.06849070E-04    3
-0.05424184E-07 0.14721313E-11 0.04507593E+06 0.09350778E+01                   4
SIH2               42489SI  1H  2           G  0300.00   3000.00  1000.00      1
 0.04142390E+02 0.02150191E-01-0.02190730E-05 0.02073725E-08 0.04741018E-12    2
 0.03110483E+06 0.02930745E+01 0.03475092E+02 0.02139338E-01 0.07672305E-05    3
 0.05217668E-08-0.09898824E-11 0.03147397E+06 0.04436585E+02                   4
SIH3               42489SI  1H  3           G  0300.00   3000.00  1000.00      1
 0.05015906E+02 0.03732750E-01-0.03609053E-05 0.03729193E-08 0.08468491E-12    2
 0.02190233E+06-0.04291368E+02 0.02946733E+02 0.06466763E-01 0.05991653E-05    3
-0.02218413E-07 0.03052669E-11 0.02270173E+06 0.07347948E+02                   4
SIH4              121386SI  1H  4           G  0300.00   4000.00  1000.00      1
 0.06893873E+02 0.04030500E-01-0.04183314E-05 0.02291394E-08 0.04384766E-12    2
 0.11070374E+04-0.01749116E+03 0.02475166E+02 0.09003721E-01 0.02185394E-04    3
-0.02681423E-07-0.06621080E-11 0.02925488E+05 0.07751014E+02                   4
SI2H2             111191H   2SI  2           G  0300.00   4000.00  1500.00      1
 0.08099063E+02 0.12942199E-02-0.02447197E-05-0.14495115E-10 0.05867240E-13    2
 0.04476428E+06-0.01877322E+03 0.09668390E+01 0.01932959E+00-0.01825421E-03    3
 0.08404012E-07-0.15372276E-11 0.04712241E+06 0.01907608E+03                   4
SI2H3              90589SI  2H  3           G  0300.00   2000.00  1000.00      1
 0.07257627E+02 0.05123859E-01-0.07633465E-05-0.06662471E-08 0.02053052E-11    2
 0.05062055E+06-0.10314127E+02 0.03335404E+02 0.02155614E+00-0.02933937E-03    3
 0.02287784E-06-0.07272827E-10 0.05146157E+06 0.08656853E+02                   4
H3SISIH           111191H   4SI  2           G  0300.00   4000.00  1500.00      1
 0.11272022E+02 0.02538145E-01-0.02998471E-05-0.09465367E-09 0.01855053E-12    2
 0.03297169E+06-0.03264598E+03 0.03698707E+02 0.01870180E+00-0.14307038E-04    3
 0.06005836E-07-0.11162929E-11 0.03590825E+06 0.08825191E+02                   4
H2SISIH2           42489SI  2H  4           G  0300.00   3000.00  1000.00      1
 0.08986817E+02 0.05405047E-01-0.05214021E-05-0.05313742E-08 0.11887266E-12    2
 0.02832747E+06-0.02004478E+03 0.05133186E+02 0.12528548E-01-0.04620421E-05    3
-0.06606075E-07 0.02864344E-10 0.02956915E+06 0.07605133E+01                   4
SI2H5              90589SI  2H  5           G  0300.00   2000.00  1000.00      1
 0.08451010E+02 0.09286371E-01-0.10911831E-05-0.14423673E-08 0.04250824E-11    2
 0.02472718E+06-0.01710331E+03 0.15788481E+01 0.03549382E+00-0.04267511E-03    3
 0.03059177E-06-0.09360425E-10 0.02630549E+06 0.16720734E+02                   4
SI2H6              90589SI  2H  6           G  0300.00   2000.00  1000.00      1
 0.08882090E+02 0.11513955E-01-0.12162159E-05-0.01905085E-07 0.05542379E-11    2
 0.05967241E+05-0.02265611E+03 0.05301921E+01 0.04184055E+00-0.04685249E-03    3
 0.03179525E-06-0.09484526E-10 0.07950597E+05 0.01880453E+03                   4
H                 120186H   1               G  0300.00   5000.00  1000.00      1
 0.02500000E+02 0.00000000E+00 0.00000000E+00 0.00000000E+00 0.00000000E+00    2
 0.02547162E+06-0.04601176E+01 0.02500000E+02 0.00000000E+00 0.00000000E+00    3
 0.00000000E+00 0.00000000E+00 0.02547162E+06-0.04601176E+01                   4
```

```
.
.
.
REACTIONS  MOLECULES  KELVINS
!
! Electron impact reactions assuming a Maxwellian EEDF:
!
 E + AR  =>  E + AR*                    1.1748E-08   4.6639E-02   1.3856E+05
     TDEP/E/      !exc,<20eV: Peuch,JPhD19:2309(1986), >20eV: Peterson,JChPh5
     EXCI/11.60/
  E + AR  =>  AR+ + 2E                  7.0708E-11   6.0983E-01   1.8712E+05
     TDEP/E/      !Peterson, JChPh 56:6068 (1972)
     EXCI/16.00/
  E + AR*  =>  AR+ + 2E                 1.2456E-07   5.0382E-02   6.0524E+04
     TDEP/E/      ! Margreiter et al., Contrib. Plasma Phys. 30:487 (1990)
     EXCI/ 4.43/
  E + O2 => O2 + E                      1.4127E-04  -1.5000E+00   1.1594E+04
     TDEP/E/      !v=0->1 resonant: Itikawa, JPhysChemRefData v18,p23, 1989
     EXCI/ 0.57/
     DUP
  E + O2 => O2 + E                      2.4096E-04  -9.3373E-01   7.6827E+04
     TDEP/E/      !vib sum:  Itikawa, JPhysChemRefData v18,p23, 1989
     EXCI/ 3.90/   !reax#5
     DUP
  E + O2 => O2 + E                      7.1298E-08  -1.4161E-01   3.0812E+04
     TDEP/E/      !elec exc a1Deltag:  Itikawa, JPhysChemRefData v18,p23, 198
     EXCI/ 0.98/   !reax#6
     DUP
  E + O2 => O2 + E                      2.7456E-10   3.2916E-02   3.0656E+04
     TDEP/E/      !elec exc b1Sigmag:  Itikawa, JPhysChemRefData v18,p23, 198
     EXCI/ 1.63/
     DUP
  E + O2 => O2 + E                      2.2885E-10   4.0187E-01   6.8652E+04
     TDEP/E/      !electronic sum:  Itikawa, JPhysChemRefData v18,p23, 1989
     EXCI/6.2/   !B3sigma+A3sigma+C3delta+c1sigma
     DUP
  E + O2 => O + O* + E                  4.5210E-13   8.7108E-01   5.1069E+04
     TDEP/E/      !Cosby, JChemPhys v98:9560 (1993); Itikawa for >200eV
     EXCI/ 5.12/
  E + O2 => O2+ + 2E                    3.9851E-14   1.1255E+00   1.3758E+05
     TDEP/E/      !Itikawa, JPhysChemRefData v18,p23, 1989
     EXCI/12.06/
  E + O2 => O + O-                      3.6044E-08  -5.2403E-01   5.7440E+04
     TDEP/E/      !Itikawa, JPhysChemRefData v18,p23, 1989
     EXCI/ 0.03/
  E + O => O* + E                       4.2983E-07  -3.4465E-01   3.8431E+04
     TDEP/E/      ! O_exc_1D: Itikawa,  JPhysChemRefData, v19,p637, 1990
     EXCI/ 4./   !reax#11 (O*)
  E + O => O + E                        1.2447E-09  -1.7434E-02   6.0440E+04
     TDEP/E/      ! O_exc_1S: Itikawa,  JPhysChemRefData, v19,p637, 1990
     EXCI/ 4.18/
     DUP
  E + O => O + E                        1.6713E-09   2.9276E-02   1.4694E+05
     TDEP/E/      !3's3 D0 exc: Itikawa, JPhysChemRefData, v19,p637, 1990
     EXCI/13.00/
     DUP
  E + O => O + E                        4.3591E-09  -8.3646E-03   1.1015E+05
     TDEP/E/      !3s3 S0 exc: Itikawa, JPhysChemRefData, v19,p637, 1990
     EXCI/ 9.00/
     DUP
  E + O => O + E                        1.9285E-15   1.0645E+00   5.3078E+05
     TDEP/E/      !dbl ioniz rate: Thompson, JPhysB 28:1321, 1995
     EXCI/48.77/
     DUP
  E + O => O+ + 2E                      1.9509E-11   6.2331E-01   1.6541E+05
     TDEP/E/      ! Itikawa, JPhysChemRefData, v19,p637, 1990
     EXCI/13.61/
  E + O* => O+ + 2E                     1.9509E-11   6.2331E-01   1.40E+05
     TDEP/E/      ! Estimated from ground-state reax, multiply C*11.6/13.61
     EXCI/11.6/
  E + O- => O + 2E                      2.0976E-10   5.4384E-01   3.9434E+04
     TDEP/E/      !Detachment:  Peart, B., J Phys B, v12, p2735, 1979. !guess
     EXCI/ 3.00/
  E + E + O => O- + E                   1.e-30       0.0          0.0
     TDEP/E/      !Itikawa,  JPhysChemRefData, v19,p637, 1990; detailed
balancing
!-----------------------------------------------------------------------------
! Ion and metastable reactions for Ar-O2 only
!-----------------------------------------------------------------------------
 AR* + AR* => AR + AR+ + E     6.2E-10    0.0    0.0 !Lee's thesis
 O- + O2+     => O + O2        2.8e-7     0.0    0.   !EM estimate
    TDEP/O-/
 O- + O+      => 2O            2.8e-7     0.0    0.   !Olson
    TDEP/O-/
 O- + O => O2 + E              1.4E-10    0.0    0.0
    TDEP/O-/          !   Steinfeld, JPhysChemRefData 16, 911 (1987)
 O- + AR+ => O + AR            2.8E-7     0.0    0.0 !est same as O- + O+
    TDEP/AR+/
 O+ + O2 => O2+ + O            2.10E-11   0.     0.
    TDEP/O+/          !   Anicich, JPhChRD 22:1469,1993
 O2+ + AR => AR+ + O2          5.50E-11   0.     0.
    TDEP/O2+/         !   Anicich, JPhChRD 22:1469,1993, estimated like Xenon
```

Figure 17. Listing of the beginnings of the thermo data and the reactions sections of the CHEMKIN chemistry input file for example problem 2.

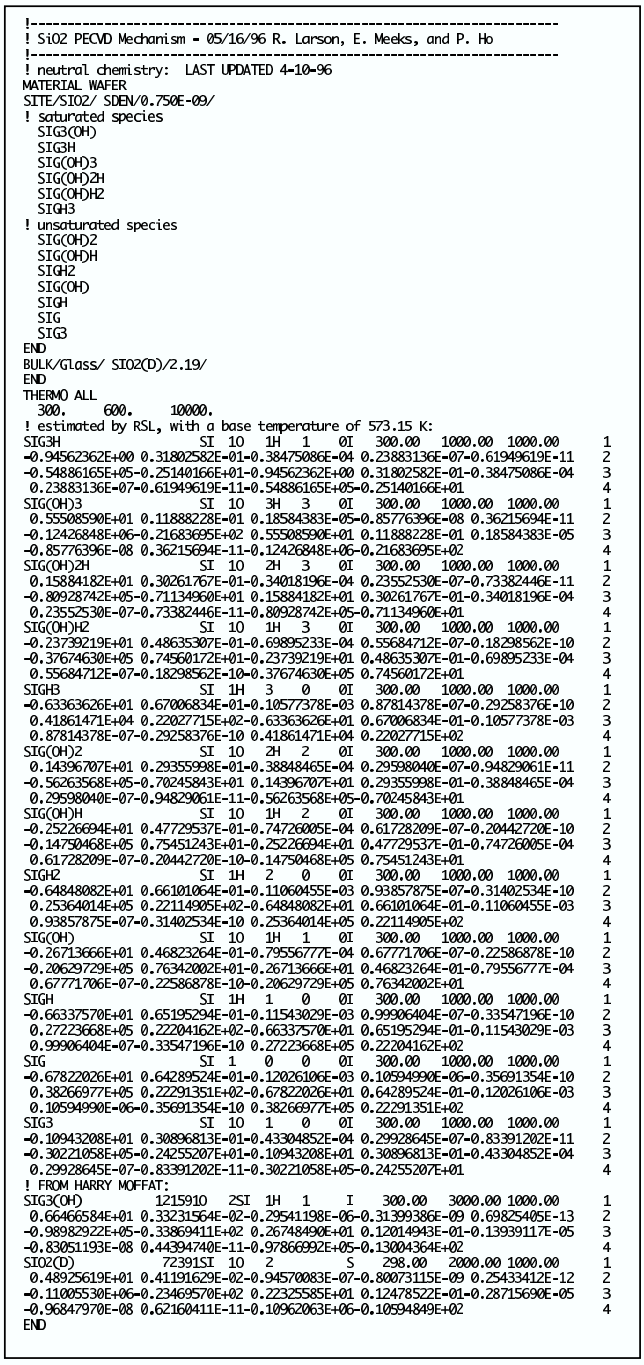

```
!-----------------------------------------------------------------------
! SiO2 PECVD Mechanism - 05/16/96 R. Larson, E. Meeks, and P. Ho
!-----------------------------------------------------------------------
! neutral chemistry:  LAST UPDATED 4-10-96
MATERIAL WAFER
SITE/SIO2/ SDEN/0.750E-09/
! saturated species
  SIG3(OH)
  SIG3H
  SIG(OH)3
  SIG(OH)2H
  SIG(OH)H2
  SIGH3
! unsaturated species
  SIG(OH)2
  SIG(OH)H
  SIGH2
  SIG(OH)
  SIGH
  SIG
  SIG3
END
BULK/Glass/ SIO2(D)/2.19/
END
THERMO ALL
  300.     600.     10000.
! estimated by RSL, with a base temperature of 573.15 K:
SIG3H                 SI  1O   1H   1    0I   300.00   1000.00  1000.00      1
-0.94562362E+00 0.31802582E-01-0.38475086E-04 0.23883136E-07-0.61949619E-11    2
-0.54886165E+05-0.25140166E+01-0.94562362E+00 0.31802582E-01-0.38475086E-04    3
 0.23883136E-07-0.61949619E-11-0.54886165E+05-0.25140166E+01                   4
SIG(OH)3              SI  1O   3H   3    0I   300.00   1000.00  1000.00      1
 0.55508590E+01 0.11888228E-01 0.18584383E-05-0.85776396E-08 0.36215694E-11    2
-0.12426848E+06-0.21683695E+02 0.55508590E+01 0.11888228E-01 0.18584383E-05    3
-0.85776396E-08 0.36215694E-11-0.12426848E+06-0.21683695E+02                   4
SIG(OH)2H             SI  1O   2H   3    0I   300.00   1000.00  1000.00      1
 0.15884182E+01 0.30261767E-01-0.34018196E-04 0.23552530E-07-0.73382446E-11    2
-0.80928742E+05-0.71134960E+01 0.15884182E+01 0.30261767E-01-0.34018196E-04    3
 0.23552530E-07-0.73382446E-11-0.80928742E+05-0.71134960E+01                   4
SIG(OH)H2             SI  1O   1H   3    0I   300.00   1000.00  1000.00      1
-0.23739219E+01 0.48635307E-01-0.69895233E-04 0.55684712E-07-0.18298562E-10    2
-0.37674630E+05 0.74560172E+01-0.23739219E+01 0.48635307E-01-0.69895233E-04    3
 0.55684712E-07-0.18298562E-10-0.37674630E+05 0.74560172E+01                   4
SIGH3                 SI  1H   3    0    0I   300.00   1000.00  1000.00      1
-0.63363626E+01 0.67006834E-01-0.10577378E-03 0.87814378E-07-0.29258376E-10    2
 0.41861471E+04 0.22027715E+02-0.63363626E+01 0.67006834E-01-0.10577378E-03    3
 0.87814378E-07-0.29258376E-10 0.41861471E+04 0.22027715E+02                   4
SIG(OH)2              SI  1O   2H   2    0I   300.00   1000.00  1000.00      1
 0.14396707E+01 0.29355998E-01-0.38848465E-04 0.29598040E-07-0.94829061E-11    2
-0.56263568E+05-0.70245843E+01 0.14396707E+01 0.29355998E-01-0.38848465E-04    3
 0.29598040E-07-0.94829061E-11-0.56263568E+05-0.70245843E+01                   4
SIG(OH)H              SI  1O   1H   2    0I   300.00   1000.00  1000.00      1
-0.25226694E+01 0.47729537E-01-0.74726005E-04 0.61728209E-07-0.20442720E-10    2
-0.14750468E+05 0.75451243E+01-0.25226694E+01 0.47729537E-01-0.74726005E-04    3
 0.61728209E-07-0.20442720E-10-0.14750468E+05 0.75451243E+01                   4
SIGH2                 SI  1H   2    0    0I   300.00   1000.00  1000.00      1
-0.64848082E+01 0.66101064E-01-0.11060455E-03 0.93857875E-07-0.31402534E-10    2
 0.25364014E+05 0.22114905E+02-0.64848082E+01 0.66101064E-01-0.11060455E-03    3
 0.93857875E-07-0.31402534E-10 0.25364014E+05 0.22114905E+02                   4
SIG(OH)               SI  1O   1H   1    0I   300.00   1000.00  1000.00      1
-0.26713666E+01 0.46823264E-01-0.79556777E-04 0.67771706E-07-0.22586878E-10    2
-0.20629729E+05 0.76342002E+01-0.26713666E+01 0.46823264E-01-0.79556777E-04    3
 0.67771706E-07-0.22586878E-10-0.20629729E+05 0.76342002E+01                   4
SIGH                  SI  1H   1    0    0I   300.00   1000.00  1000.00      1
-0.66337570E+01 0.65195294E-01-0.11543029E-03 0.99906404E-07-0.33547196E-10    2
 0.27223668E+05 0.22204162E+02-0.66337570E+01 0.65195294E-01-0.11543029E-03    3
 0.99906404E-07-0.33547196E-10 0.27223668E+05 0.22204162E+02                   4
SIG                   SI  1    0    0    0I   300.00   1000.00  1000.00      1
-0.67822026E+01 0.64289524E-01-0.12026106E-03 0.10594990E-06-0.35691354E-10    2
 0.38266977E+05 0.22291351E+02-0.67822026E+01 0.64289524E-01-0.12026106E-03    3
 0.10594990E-06-0.35691354E-10 0.38266977E+05 0.22291351E+02                   4
SIG3                  SI  1O   1    0    0I   300.00   1000.00  1000.00      1
-0.10943208E+01 0.30896813E-01-0.43304852E-04 0.29928645E-07-0.8339120ZE-11    2
-0.30221058E+05-0.24255207E+01-0.10943208E+01 0.30896813E-01-0.43304852E-04    3
 0.29928645E-07-0.83391202E-11-0.30221058E+05-0.24255207E+01                   4
! FROM HARRY MOFFAT:
SIG3(OH)          1215910   2SI  1H   1     I    300.00   3000.00 1000.00      1
 0.66466584E+01 0.33231564E-02-0.29541198E-06-0.31399386E-09 0.69825405E-13    2
-0.98982922E+05-0.33869411E+02 0.26748490E+01 0.12014943E-01-0.13939117E-05    3
-0.83051193E-08 0.44394740E-11-0.97866992E+05-0.13004364E+02                   4
SIO2(D)           72391SI  1O   2    S    298.00   2000.00 1000.00      1
 0.48925619E+01 0.41191629E-02-0.94570083E-07-0.80073115E-09 0.25433412E-12    2
-0.11005530E+06-0.23469570E+02 0.22325585E+01 0.12478522E-01-0.28715690E-05    3
-0.96847970E-08 0.62160411E-11-0.10962063E+06-0.10594849E+02                   4
END
```

```
REACTIONS MWOFF MOLECULES KELVIN
! deposition of silicon-containing radicals (since the surface is cold,
!   deposition of saturated species will be very slow; also, possible
!   substrates other than SIG3(OH) are assumed to be converted by
!   intramolecular reactions or saturated by attachment of gas-phase
!   radicals)
! Note 8/6/96:  Made deposition reactions irreversible.
SIH3 + SIG3(OH) => SIGH2 + SIO2(D) + H2       1.0         0.          0.
   STICK
SIH2 + SIG3(OH) => SIGH + SIO2(D) + H2        1.0         0.          0.
   STICK
SIH + SIG3(OH) => SIG + SIO2(D) + H2          1.0         0.          0.
   STICK
SI + SIG3(OH) => SIGH + SIO2(D)               1.0         0.          0.
   STICK  !added by EM 12-04-96
SIO + SIG3(OH) => SIG(OH) + SIO2(D)           1.0         0.          0.
   STICK  ! making this reversible makes a big difference at high T
HSIO + SIG3(OH) => SIG(OH)H + SIO2(D)         1.0         0.          0.
   STICK
SIH3O + SIG3(OH) => SIGH3 + SIO2(D) + OH      1.0         0.          0.
   STICK
! direct deposition of SiO2
SIO2 => SIO2(D)                               1.0         0.          0.
   STICK
! intramolecular elimination of H2 (should be ion-enhanced)
SIG(OH)2H = SIG3(OH) + H2                     2.000E+10   0.      15000.
SIG(OH)H2 = SIG3H + H2                        2.000E+10   0.      15000.
SIG(OH)H = SIG3 + H2                          2.000E+10   0.      15000.
! intramolecular elimination of H2O (should be ion-enhanced)
SIG(OH)3 = SIG3(OH) + H2O                     2.000E+10   0.      15000.
SIG(OH)2H = SIG3H + H2O                       2.000E+10   0.      15000.
SIG(OH)2 = SIG3 + H2O                         2.000E+10   0.      15000.
! oxidation of surface hydrogens
SIG3H + O = SIG3(OH)                          0.40   0.0   0.0
   STICK
SIG(OH)2H + O = SIG(OH)3                      0.40   0.0   0.0
   STICK
SIG(OH)H2 + O = SIG(OH)2H                     0.40   0.0   0.0
   STICK
SIGH3 + O = SIG(OH)H2                         0.40   0.0   0.0
   STICK
SIG(OH)H + O = SIG(OH)2                       0.40   0.0   0.0
   STICK
SIGH2 + O = SIG(OH)H                          0.40   0.0   0.0
   STICK
SIGH + O = SIG(OH)                            0.40   0.0   0.0
   STICK
! copy above reactions for O*
SIG3H + O* = SIG3(OH)                         0.40   0.0   0.0
   STICK
SIG(OH)2H + O* = SIG(OH)3                     0.40   0.0   0.0
   STICK
SIG(OH)H2 + O* = SIG(OH)2H                    0.40   0.0   0.0
   STICK
SIGH3 + O* = SIG(OH)H2                        0.40   0.0   0.0
   STICK
SIG(OH)H + O* = SIG(OH)2                      0.40   0.0   0.0
   STICK
SIGH2 + O* = SIG(OH)H                         0.40   0.0   0.0
   STICK
SIGH + O* = SIG(OH)                           0.40   0.0   0.0
   STICK
! attachment of H atoms to dangling bonds
SIG(OH)2 + H = SIG(OH)2H                      1.0         0.          0.
   STICK
SIG(OH)H + H = SIG(OH)H2                      1.0         0.          0.
   STICK
SIGH2 + H = SIGH3                             1.0         0.          0.
   STICK
SIG(OH) + H = SIG(OH)H                        1.0         0.          0.
   STICK
SIGH + H = SIGH2                              1.0         0.          0.
   STICK
SIG + H = SIGH                                1.0         0.          0.
   STICK
SIG3 + H = SIG3H                              1.0         0.          0.
   STICK
! attachment of OH radicals to dangling bonds
SIG(OH)2 + OH = SIG(OH)3                      1.0         0.          0.
   STICK
SIG(OH)H + OH = SIG(OH)2H                     1.0         0.          0.
   STICK
SIGH2 + OH = SIG(OH)H2                        1.0         0.          0.
   STICK
SIG(OH) + OH = SIG(OH)2                       1.0         0.          0.
   STICK
```

Figure 18. Listing of the first 170 lines (of 580) from the Surface CHEMKIN input file for example problem 2.

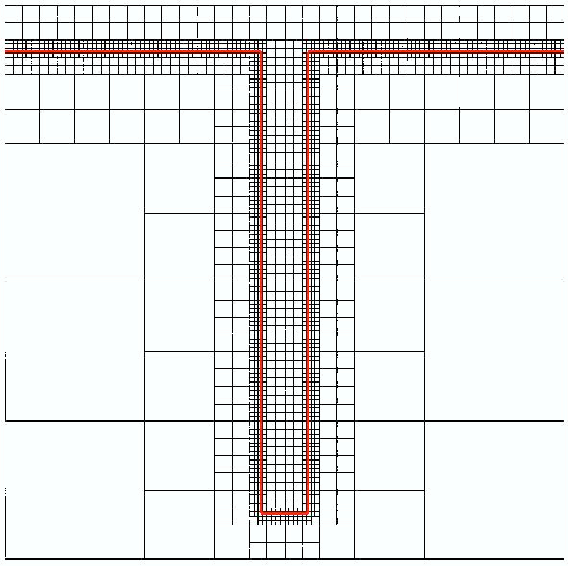

(a) Initial surface geometry and refined level-set grid used in the 2D PECVD example problem.

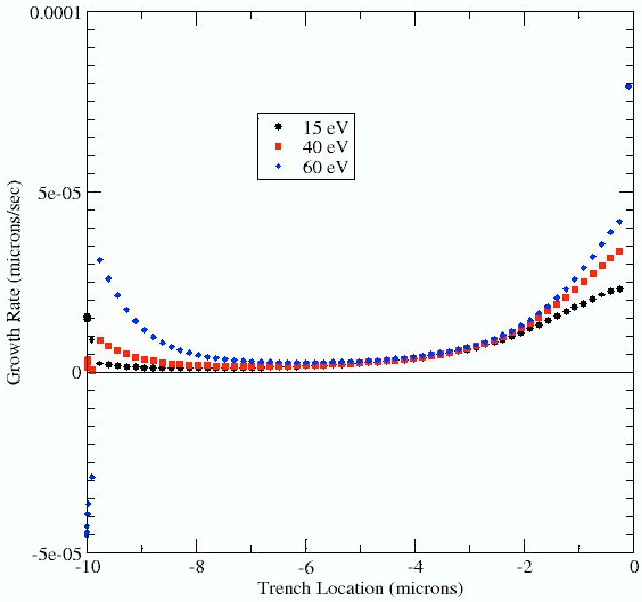

(b) Initial growth rate as a function of depth and ion energy in the 2D PECVD example problem.

Figure 19. Sample output from example ChISELS model of PECVD of SiO_2 from Ar, O_2 and SiH_4

4.4.3 Silane Deposition in a Simple 3-D Square Hole

This example illustrates the solution of a simple 3D deposition problem that is analogous to example 1 except that the initial geometry is a square hole. The chemistry corresponds to LPCVD of undoped silicon from a silane precursor, and the thermodynamic conditions and chemical mechanism being modeled are also identical to those in example 1. The input command file and the associated geometry input file "in.geom_notch3d" are listed in Figure 20. Note that for 3-D problems, each line in the geometry input file defines a unique triangular-shaped surface element. One difference to note is that the surface orientation of this problem is different – in this geometry the source surface is defined as "5", corresponding to the maximum z coordinate in the computational domain.

Sample output from this problem is shown in Figure 21. Note the difference between the initially specified surface geometry shown in (a) with the meshed surface at time t = 0 shown in (b). Edges and corners cannot be represented exactly in the discrete representation but are approximated as shown based on the relatively coarse mesh resolution specified here. Figures 21(c) and (d) show results at two later points in time, illustrating that even uniform deposition processes can yield fairly complex 3-D surface topologies.

```
# Input Command file for Silane deposition in
# a simple 3-D square hole
#
# Problem Definition Commands
# -----------------------------------------
dimension              3
initial surfaces       in.geom_notch3d
chemkin input          smallche.inp
surface chemkin input  smallsur.inp
number gas species     3
mole fraction          SIH4   1.0
mole fraction          SIH2   0.0
mole fraction          H2     0.0

temperature            853.0  0.0  0.0
gas pressure           0.4

# Time Step and Run-time controls
# -----------------------------------------
timestep               900.0
adjust dt flag         0
number of steps        20

# Output Controls
# -----------------------------------------
qt output              1
cell output            1
qt_filename            out.geom_notch3d
screen                 2

# Modeling Controls and Specifications
# -----------------------------------------
global box             0.0 0.0 0.0 6.0 6.0 6.0
source side            5
grid levels            5
```

(a) Input command file

```
# Initial Surface definition for Silane
# deposition in a simple 3-D square hole
# (Values in microns)
#
#    X1 Y1 Z1 X2 Y2 Z2 X3 Y3 Z3  Ni  Nj  Nk
1 0  0. 0. 2. 0. 2. 2. 2. 2. 2.  0.0 0.0 1.0
2 0  0  0. 2. 2. 2. 2. 2. 0. 2.  0.0 0.0 1.0
3 0  2. 0. 2. 2. 2. 2. 4. 2. 2.  0.0 0.0 1.0
4 0  2. 0. 2. 4. 2. 2. 4. 0. 2.  0.0 0.0 1.0
5 0  4. 0. 2. 4. 2. 2. 6. 2. 2.  0.0 0.0 1.0
6 0  4. 0. 2. 6. 2. 2. 6. 0. 2.  0.0 0.0 1.0
7 1  0. 2. 2. 0. 4. 2. 2. 4. 2.  0.0 0.0 1.0
8 1  0. 2. 2. 2. 4. 2. 2. 2. 2.  0.0 0.0 1.0
9 1  2. 2. 1. 2. 4. 1. 4. 4. 1.  0.0 0.0 1.0
10 1 2. 2. 1. 4. 4. 1. 4. 2. 1.  0.0 0.0 1.0
11 1 4. 2. 2. 4. 4. 2. 6. 4. 2.  0.0 0.0 1.0
12 1 4. 2. 2. 6. 4. 2. 6. 2. 2.  0.0 0.0 1.0
13 2 0. 4. 2. 0. 6. 2. 2. 6. 2.  0.0 0.0 1.0
14 2 0. 4. 2. 2. 6. 2. 2. 4. 2.  0.0 0.0 1.0
15 2 2. 4. 2. 2. 6. 2. 4. 6. 2.  0.0 0.0 1.0
16 2 2. 4. 2. 4. 6. 2. 4. 4. 2.  0.0 0.0 1.0
17 2 4. 4. 2. 4. 6. 2. 6. 6. 2.  0.0 0.0 1.0
18 2 4. 4. 2. 6. 6. 2. 6. 4. 2.  0.0 0.0 1.0
19 3 2. 2. 2. 2. 4. 2. 2. 4. 1.  1.0 0.0 0.0
20 3 2. 2. 2. 2. 4. 1. 2. 2. 1.  1.0 0.0 0.0
21 3 2. 4. 2. 4. 4. 2. 4. 4. 1.  0.0 -1.0 0.0
22 3 2. 4. 2. 4. 4. 1. 2. 4. 1.  0.0 -1.0 0.0
23 3 4. 4. 2. 4. 2. 2. 4. 2. 1. -1.0 0.0 0.0
24 3 4. 4. 2. 4. 2. 1. 4. 4. 1. -1.0 0.0 0.0
25 4 4. 2. 2. 2. 2. 2. 2. 2. 1.  0.0 1.0 0.0
26 4 4. 2. 2. 2. 2. 1. 4. 2. 1.  0.0 1.0 0.0
```

(b) Geometry Input file

Figure 20. Listing of the main input file and the geometry input file for example problem 3.

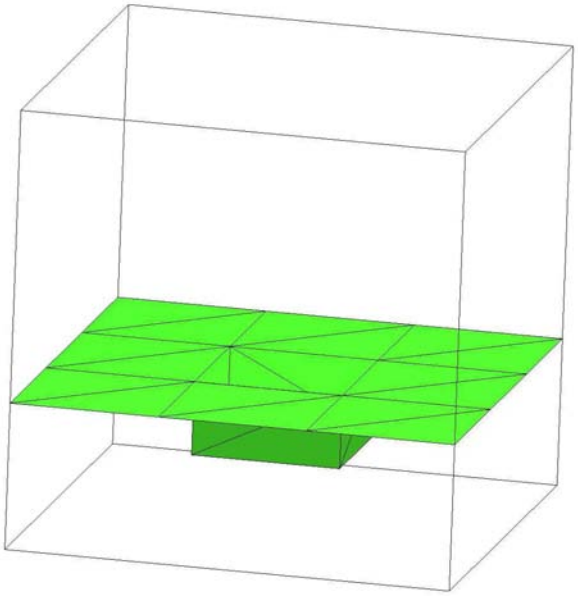

a. Initial surface specified by input.

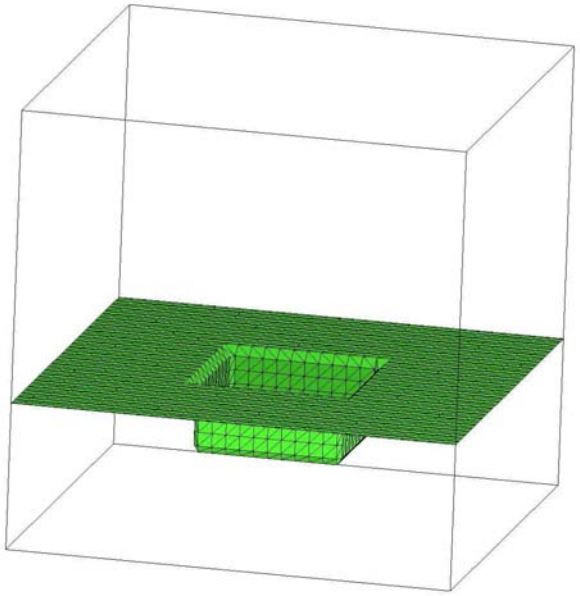

b. Meshed surface at t = 0 min.

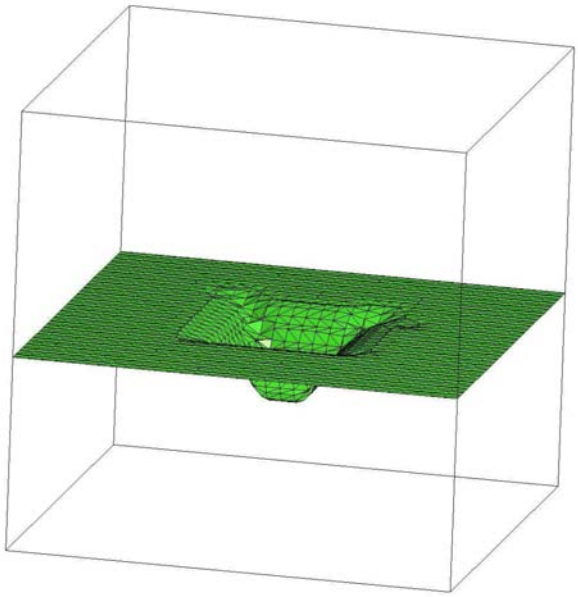

c. Meshed surface at t = 150 min.

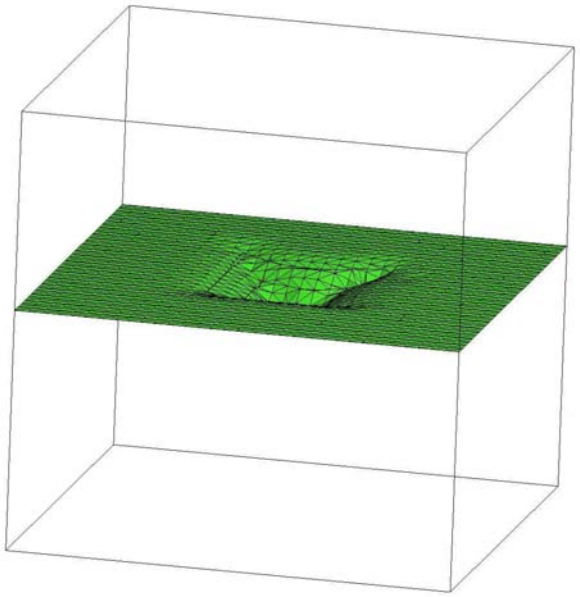

d. Meshed surface at t = 300 min.

Figure 21. Sample output from Silane deposition in a simple 3-D square hole.

References

[1] John Strain. Semi-lagrangian methods for level-set equations. *Journal of Computational Physics*, 1999.

[2] R. J. Kee, F. M. Rupley, J. A. Miller, M. E. Coltrin, J. F. Grcar, E. Meeks, H. K. Moffat, A. E. Lutz, G. Dixon-Lewis, M. D. Smooke, J. Warnatz, G. H. Evans, R. S. Larson, R. E. Mitchell, L. R. Petzold, W. C. Reynolds, M. Caracotsios, W. E. Stewart, P. Glarborg, C. Wang, C. L. McLellan, O. Adigun, W. G. Houf, C. P. Chou, S. F. Miller, P. Ho, P. D. Young, and D. J. Young. Chemkin, release 4.0.2. Reaction Design, San Diego, CA, 2005.

[3] M. E. Coltrin, R. J. Kee, F. M. Rupley, and E. Meeks. SURFACE CHEMKIN III: A Fortran Package for Analyzing Heterogeneous Chemical Kinetics at a Solid-Surface - Gas-Phase Interface. Report No. SAND96-8217, Sandia National Laboratories, 1996.

[4] M. S. Rodgers and J. J. Sniegowski. Designing microelectromechanical systems-on-a-chip in a 5-level surface micromachine technology. *2nd Int. Conf. Eng. Design and Automation*, 1998.

[5] Timothy S. Cale, Tushar P. Merchant, Leonard J. Borucki, and Andrew H. Labun. Topography simulation for the virtual wafer fab. *Thin Solid Films*, 365:152–175, 2000.

[6] A. H. Labun, H. K. Moffat, and T. S. Cale. Mechanistic feature-scale profile simulation of SiO_2 low-pressure chemical vapor deposition by tetraethoxysilane pyrolysis. *J. Vac. Sci. Technol. B.*, 18:267–278, 2000.

[7] J. A. Sethian. *Level Set Methods and Fast Marching Methods*. Cambridge University Press, New York, USA, 1999.

[8] T. S. Cale and V. Mahadev. Feature scale transport and reaction during low-pressure deposition processes. In S. Rossnagel, editor, *Thin Films*, volume 22, pages 175–277. Academic Press, 1996.

[9] M. W. Glass. CHAPARRAL: A library for solving large enclosure radiation heat transfer problems. Report No. SAND95-2049, Sandia National Laboratories, 1995.

[10] R. B. Walker. http://www.t12.lanl.gov/home/toposim.

[11] R. B. Walker and J. D. Kress. Toposim-3D: A 3D feature-scale profile simulation tool. MRS Workshop on Advances in Thin Film Simulations and Experimental Verification, 1999.

[12] T. S. Cale. EVOLVE is a deposition, etch, and thin film flow simulator, developed under the direction of Timothy S. Cale. Version 5.0b released in November, 1998.

[13] P. W. Atkins. *Physical Chemistry*. W. H. Freeman and Company, New York, 1990.

[14] B. Chapman. *Glow Discharge Processes: Sputtering and Plasma Etching*. Wiley-InterScience, 1980.

[15] Brian Gavin Higgins. *Capillary Hydrodynamics and Coating Beads*. PhD thesis, University of Minnesota., 1980. Published by University Microfilms International, Ann Arbor, MI.

[16] W. Noh and P. Woodward. A simple line interface calculation. In *Fifth International Conference on Fluid Dynamics*, 1976.

[17] Stanley Osher and Ronald P. Fedkiw. Levelset methods: An overview and some recent results. *J. Comp. Phys*, 169:463–502, 2001.

[18] R. S. Tuminaro, M. Heroux, S. A. Hutchinson, and J. N. Shadid. Official Aztec User's Guide: Version 2.1. Report No. SAND99-8801J, Sandia National Laboratories, 1999.

[19] Michael Bartsch, Thomas Weiland, and Martin Witting. Generation of 3D isosurfaces by means of the marching cube algorithm. *IEEE Transactions on Magnetics*, 32:1469–1472, 1996.

[20] P. S. Pacheco. *Parallel Programming with MPI*. Morgan Kaufmann Publishers, Inc., San Francisco, CA, USA, 1996.

[21] K. Devine, E. Boman, R. Heaphy, B. Hendrickson, and C. Vaughan. Zoltan data management services for parallel dynamic applications. *Computing in Science and Engineering*, 4(2):90–97, 2000.

[22] K. Devine, B. Hendrickson, E. Boman, M. St.John, and C. Vaughan. Zoltan: A dynamic load-balancing library for parallel applications; User's Guide. Report No. SAND99-1376, Sandia National Laboratories, 1999.

[23] http://www.trolltech.com/products.

[24] W. G. Breiland, M. E. Coltrin, and P. Ho. Comparisons between a gas-phase model of silane CVD and laser-diagnostic measurements. *Journal of Applied Physics*, 59:3267, 1986.

[25] M. E. Coltrin, R. J. Kee, and G. H. Evans. A mathematical model of the fluid mechanics and gas-phase chemistry in a rotating disk CVD reactor. *Journal of Electrochemical Society*, 136:819, 1989.

[26] W. G. Breiland and M. E. Coltrin. Si deposition rates in a two-dimensional CVD reactor and comparisons with model calculations. *J. Electrochem. Soc.*, 137:2313, 1990.

[27] W. G. Houf, J. F. Grcar, and W. G. Breiland. A model for low pressure CVD in a hot-wall tubular reactor. *Mater. Sci. and Eng.*, B17:163–171, 1993.

[28] P Ho, M. E. Coltrin, and W. G. Breiland. Laser-induced fluorescence measurements and kinetic analysis of si atom formation in a rotating disk chemical deposition reactor. *J. Phys. Chem*, 98:10138–10147, 1994.

[29] E. Meeks, R. S. Larson, P. Ho, C. Apblett, S. M. Han, E. Edelberg, and E. S. Aydil. Modeling of SiO_2 deposition in high density plasma reactors and comparisons of model predictions with experimental measurements. *J. Vac. Sci. Technol. A.*, 16:544–563, 1998.

DISTRIBUTION:

1 Ellen Meeks
Reaction Design
6440 Lusk Boulevard, Suite D-205
San Diego, CA 92121

1 John Garrison
Reaction Design
6440 Lusk Boulevard, Suite D-205
San Diego, CA 92121

1 Jeff Bailey
Aviza Technologies
440 Kings Village Rd.
Scotts Valley, CA 95066

1 Robert B. Walker
Los Alamos National Laboratory
Group T-12, MS B268
Los Alamos, NM 87545

1 Ray Myers
Elemental Technologies
301 East 925 North
American Fork, UT 84003

5 MS 0316
Lawrence C. Musson, 1437

5 MS 0316
Rodney C. Schmidt, 1437

1 MS 0316
Scott Hutchinson, 1437

1 MS 0321
Jennifer Nelson, 1430

2 MS 0734
Pauline Ho, 6215

1 MS 0734
Bruce Kelley, 6215

1 MS 0741
Rush Robinett, 6210

1 MS 0824
Wahid Hermina, 1510

1 MS 0826
C. Channy Wong, 1513

1 MS 1110
Steve Plimpton, 1412

1 MS 1069
Vic Yarberry, 1737

1 MS 1077
Rob Jarecki, 1747

1 MS 1077
Tom Zipperian, 1740

1 MS 1080
Dave Sandison, 1749

1 MS 1080
Greg Bogart, 1749

1 MS 1080
Sita Mani, 1749

1 MS 1084
Dale Hetherington, 1746

1 MS 1085
Randy Shul, 1742

1 MS 1085
Charles Sullivan, 1742

1 MS 1086
Michael Coltrin, 1126

1 MS 1243
Steve Kempka, 5535

1 MS 1316
Mark Rintoul, 1412

1 MS 1322
Sudip Dosanjh, 1420

1 MS 1411
Corbett Battaile, 1814

2 MS 9018
Central Technical Files, 8944

2 MS 0899
Technical Library, 4536